Analysis of genetic networks regulating refractive eye development in collaborative cross progenitor strain mice reveals new genes and pathways underlying human myopia

Short title: Evolutionary conserved genetic networks regulate refractive eye development in mice and humans

Tatiana V. Tkatchenko[1], Rupal L. Shah[2], Takayuki Nagasaki[1], CREAM Consortium[3], UK Biobank Eye and Vision Consortium[4], and Andrei V. Tkatchenko[1,5*]

[1]Department of Ophthalmology, Columbia University, New York, New York, USA

[2]School of Optometry & Vision Sciences, Cardiff University, Cardiff, UK

[3]A full list of the CREAM members and their affiliations appear in the Supporting Information

[4]A full list of the UK Biobank Eye and Vision Consortium members and their affiliations appear in the Supporting Information

[5]Department of Pathology and Cell Biology, Columbia University, New York, New York, USA

***Correspondence to:** Andrei V. Tkatchenko, Edward S. Harkness Eye Institute Research Annex, Room 415, 635 W. 165th Street, New York, NY 10032, United States. Phone: 212-342-5135; Fax: 212-342-0094; E-mail: avt2130@cumc.columbia.edu

Abstract

Population studies suggest that genetic factors play an important role in refractive error development; however, the precise role of genetic background and the composition of the signaling pathways underlying refractive eye development remain poorly understood. Here, we analyzed normal refractive development and susceptibility to form-deprivation myopia in the eight progenitor mouse strains of the Collaborative Cross (CC). Genetic background strongly influenced both baseline refractive development and susceptibility to environmentally-induced myopia. Baseline refractive errors ranged from -21.2 diopters (D) in 129S1/svlmj mice to +22.0 D in CAST/EiJ mice and represented a continuous distribution typical of a quantitative genetic trait. The extent of induced form-deprivation myopia ranged from -5.6 D in NZO/HILtJ mice to -20.0 D in CAST/EiJ mice and also followed a continuous distribution. Whole-genome (RNA-seq) gene expression profiling in retinae from CC progenitor strains identified genes whose expression level correlated with either baseline refractive error or susceptibility to myopia. Expression levels of 2,302 genes correlated with the baseline refractive state of the eye, whereas 1,917 genes correlated with susceptibility to induced myopia. Genome-wide gene-based association analysis in the CREAM and UK Biobank human cohorts revealed that 985 of the above genes were associated with refractive error development in humans, including 847 genes which were implicated in the development of human myopia for the first time. Although the gene sets controlling baseline refractive development and those regulating susceptibility to myopia overlapped, these two processes appeared to be controlled by largely distinct sets of genes. Comparison with data for other animal models of myopia revealed that the genes identified in this study comprise a well-defined set of retinal signaling pathways, which are highly conserved across different species. These results provide attractive targets for the development of anti-myopia drugs.

Author Summary

Several lines of evidence suggest that variations in genetic background have a strong impact on a default (baseline) trajectory of eye growth and refractive development. Many studies also highlighted differences in susceptibility of different individuals to environmentally induced changes in refractive eye development, suggesting that genetic background plays an important role in visual regulation of eye growth. However, genes and signaling pathways that control the baseline trajectory of refractive eye development and those that regulate the impact of visual environment on refractive eye development are still poorly understood. Our data suggest that both processes are regulated by elaborate retinal genetic networks. Surprisingly, we found that although genes that control baseline refractive eye development and genes regulating the impact of visual environment on refractive development overlap, there is a large number of genes and pathways which exclusively control either the baseline trajectory of refractive eye development or the impact of visual environment on refractive development. Moreover, we found that many of the genes and pathways, which we found to be associated with either baseline refractive development or susceptibility to environmentally induced myopia in mice, are also associated with refractive error development in the human population and are highly conserved across different species. Identification of genes and pathways that underlie visual regulation of eye growth versus genes and pathways that control default trajectory of refractive eye development sheds light on the basic mechanisms of eye emmetropization and provides previously unexplored possibilities for the development of new treatment options for myopia.

Introduction

Myopia is the most common ocular disorder worldwide [1]. The prevalence of myopia in the U.S. has increased from 25% to ~48% in the last 40 years [2-4]. The worldwide prevalence of myopia is predicted to increase from the current 25% to 50% in the next three decades [5], while the prevalence already exceeds 80% in several parts of Asia [6, 7]. Myopia often leads to serious blinding complications such as myopic maculopathy, retinal floaters, chorioretinal atrophy, retinoschisis, retinal tears, retinal detachment, and myopic macular degeneration [8-24]. It also represents a major risk factor for a number of other serious ocular pathologies such as cataract and glaucoma [9, 10, 25-27]. Because of the increasing prevalence, myopia is rapidly becoming one of the leading causes of vision loss in several parts of the world, and World Health Organization designated myopia as one of five priority health conditions [1, 8-10, 28].

Development of myopia is controlled by both environmental and genetic factors [29-32]. Although environmental factors, such as reading and nearwork, play a very important role in the development of myopia [33-36], genetic studies suggest that the impact of environmental factors on refractive development is determined by genetic variation in "myopia-susceptibility genes" [37]. The role of genetic background in refractive eye development is also supported by animal studies, which revealed that the extent of myopia experimentally induced in animal models is strongly influenced by genetic background [38-41]. Analysis of the size of ocular components in different strains of mice suggested a significant role of genetic background in the regulation of refractive eye development [42, 43]. Wong and Brown [44] also described significant differences in visual detection, pattern discrimination and visual acuity among different strains of mice. The contribution of genetic factors to myopia has been estimated to be as high as 70-80% [45-50], and human genetic mapping studies have identified over 270 chromosomal loci linked to myopia [51-

54]. These loci implicate genes involved in multiple cellular and biological processes related to extracellular matrix organization, eye morphogenesis, retinal signaling, and visual perception [53, 54]. Gene expression profiling studies also showed that development of myopia is accompanied by changes in gene expression in the retina, choroid, and sclera [39, 55-62]. Moreover, these studies suggested that similar biological processes underlie refractive development in animal models and humans [63].

Although these studies revealed important roles of genetic variation and gene expression in the development of refractive errors, the relationship between genetic background, gene expression and development of refractive errors remains unexplored. Here, we systematically analyzed the role of genetic background in the regulation of retinal gene expression and signaling pathways underlying refractive eye development in eight inbred strains of mice and their association with human myopia using genome-wide gene expression profiling (RNA-seq) and gene-based genome-wide association analysis in the CREAM and UK Biobank human cohorts. We found that both baseline refractive state of the eye and susceptibility to myopia are inherited as quantitative traits, demonstrating strong dependence on genetic background. Furthermore, genetic background strongly influenced expression of genes in the retina and modulated a well-defined set of signaling pathways highly conserved in chickens, mice, monkeys, and humans. Our data suggest that refractive eye development is regulated by hundreds to thousands of genes across ocular tissues and point to high evolutionary conservation of signaling pathways underlying refractive development across vertebrate species.

Results

Genetic background modulates baseline refractive eye development and susceptibility to myopia in mice

Genetic background was shown to influence the size of ocular components in mice. To investigate whether genetic differences between mice would have an impact on the baseline refractive state of the eye and susceptibility to myopia, we analyzed baseline refractive development and susceptibility to form-deprivation myopia in eight inbred strains of mice, which served as founder strains for the Collaborative Cross (CC) [64], i.e., 129S1/svlmj, A/J, C57BL/6J, CAST/EiJ, NOD/ShiLtJ, NZO/HlLtJ, PWK/PhJ, and WSB/EiJ mice.

We first measured baseline refractive errors in all eight strains at P40, i.e., when baseline refractions reach a plateau in mice [65]. We found that C57BL/6J mice were emmetropic on average (+0.3 ± 0.9 D). CAST/EiJ, NZO/HlLtJ, PWK/PhJ, and WSB/EiJ mice exhibited various degrees of hyperopia ranging from +10.6±2.2 D to +22±4.0 D, whereas A/J, NOD/ShiLtJ, and 129S1/svlmj mice developed various degrees of myopia ranging from -3.5±3.6 D to -21.2±3.9 D (S1 Table, Fig. 1A). The differences between the strains were statistically significant as revealed by ANOVA ($F(7, 145) = 429.76$, $P < 0.00001$). More importantly, the distribution of refractive errors in the CC mice was continuous, suggesting that refractive state of the eye in mice is inherited as a quantitative trait.

We then analyzed susceptibility to myopia in the same strains of mice by evaluating the extent of induced form-deprivation myopia (S2 Table, Fig. 1B). Susceptibility to form-deprivation myopia was estimated by applying a diffuser to one eye at P24 and comparing the extent of induced myopia in the form-deprived eye versus the contralateral control eye after 21 days of treatment. We found large differences in susceptibility to induced myopia between the strains (S2 Table, Fig

1B), which ranged from -5.5 ± 2.1 D in NZO/HlLtJ mice to -18.7 ± 3.1 D in CAST/EiJ mice. Other strains occupied intermediate positions between NZO/HlLtJ and CAST/EiJ mice and differences between the strains in the extent of induced myopia were statistically significant as revealed by ANOVA ($F(7, 48) = 9.8$, $P < 0.00001$). The distribution of induced refractive errors was continuous, similar to baseline refractive errors, suggesting that susceptibility to myopia was also inherited as a quantitative trait in mice. Spearman's rank-order correlation analysis showed that there was no statistically significant correlation between baseline refractive errors and the extent of induced myopia ($r_s = -0.60$, $P = 0.12$). Collectively, these data suggest that genetic background plays important role in baseline refractive development and susceptibility to environmentally induced myopia in mice and that both baseline refractive error and susceptibility to myopia are inherited as quantitative traits.

Large number of genes are involved in regulation of baseline refractive error in mice via multiple retinal biological processes and signaling pathways

To identify retinal genes influencing baseline refractive eye development in mice, we used RNA-seq to analyze gene expression in the retina of eight CC strains at P28 (an age when refractive development is progressing towards its stable plateau) (Fig 2). We found that expression of 2,302 retinal genes strongly correlated with the baseline refractive state (S3 Table, Fig 2A). Genes were organized in two distinct clusters. Expression of 793 genes comprising the first cluster was positively correlated with hyperopia, i.e., expression was increased in the strains with positive refractive errors and decreased in the strains with negative refractive errors. Conversely, expression of 1,509 genes comprising the second cluster was positively correlated with myopia, i.e., expression of these genes was increased in the mouse strains with negative refractive errors

and decreased in the strains with positive refractive errors. We observed a clear transition from the "hyperopic" gene expression pattern in CAST/EiJ and PWK/PhJ mice with highly hyperopic refractive errors to the "myopic" gene expression pattern in 129S1/svlmj mice with highly myopic refractive errors. Other strains occupied intermediate positions between these two extremes and exhibited transitional patterns of gene expression, which correlated with average baseline refractive errors in these strains.

Gene ontology analysis revealed that the 2,302 genes whose expression correlated with baseline refractive error were associated with 116 biological processes, 77 cellular components, and 69 molecular functions in the retina (S4 Table). Biological processes involved in the regulation of baseline refractive development ranged from regulation of neurogenesis and neuron migration to regulation of DNA methylation, visual perception, and synaptic vesicle endocytosis. Figure 2B shows the top 15 biological processes associated with these genes, including regulation of protein kinase B, regulation of transcription and translation, covalent chromatin modification, insulin receptor signaling, dendrite morphogenesis, and response to oxidative stress, among others. Genes underlying baseline refractive development were also associated with multiple canonical signaling pathways in the retina (S5 Table, Fig 2C). Negative refractive errors were associated with activation of mTOR, EIF2, AMPK, β-adrenergic, and dopamine-DARPP32 feedback signaling pathways and suppression of HIPPO and RhoGDI signaling pathways, among others. Taken together, these data suggest that refractive eye development is regulated by a large number of genes and pathways. In summary, the development of hyperopic and myopic refractive errors was associated with specific patterns of gene expression, and the activation or suppression of many retinal signaling pathways.

Large number of genes are involved in regulation of susceptibility to myopia in mice via multiple retinal biological processes and signaling pathways

We found that genetic background influences susceptibility to experimentally induced myopia in mice and that susceptibility to myopia appears to be controlled as a quantitative trait by multiple genes (Fig 1B). To identify genes underlying inter-strain differences in susceptibility to myopia in mice, we analyzed gene expression in the retina of the eight CC strains upon induction of form-deprivation myopia at the whole-genome level, using RNA-seq (Fig 3). We found that expression of 1,917 genes strongly correlated with the extent of form-deprivation myopia in different strains of mice (S6 Table, Fig 3A). Similar to what we found with baseline refractive errors, these genes were organized in two clusters. Expression of 643 genes comprising the first cluster was positively correlated with the susceptibility to myopia, whereas expression of 1,274 genes in the second cluster was negatively correlated with the susceptibility to myopia. We found that there was a transition from a "high susceptibility" gene expression pattern in CAST/EiJ mice, which developed -18.7 ± 3.1 D of myopia, to a "low susceptibility" gene expression pattern in NZO/HlLtJ mice, in which only -5.5 ± 2.1 D of myopia was induced by visual form deprivation. Other strains exhibited transitional gene expression patterns, which correlated with the extent of induced myopia.

Gene ontology analysis suggested that 55 biological processes, 61 cellular components, and 41 molecular functions were associated with the 1,917 genes correlated with susceptibility to myopia (S7 Table). Figure 3B shows the top 15 biological processes involved in the regulation of susceptibility to myopia, including regulation of signal transduction, cell-cell adhesion, transcription, translation, protein transport, and lysosome organization, among others. Analysis of the canonical pathways influenced by the genes correlated with susceptibility to myopia revealed that increased susceptibility to myopia was associated with suppression of mTOR signaling, EIF2

signaling, protein kinase A signaling, D-myo-inositol-5-phosphate metabolism, cholesterol and choline biosynthesis, as well as with activation of amyloid processing, HIPPO signaling, PTEN signaling, and PPARα/RXRα signaling pathways (S8 Table, Fig 3C). Collectively, these data implicate an elaborate retinal genetic network and multiple signaling pathways in the regulation of susceptibility to myopia in mice.

Baseline refractive eye development and susceptibility to myopia in mice are regulated via overlapping but largely distinct retinal genetic networks

To estimate the relative contribution of genes whose expression level correlated with baseline refractive error versus susceptibility to myopia, we analyzed the overlap between the two gene sets (Fig 4). We found that 714 genes were correlated with both baseline refractive development and susceptibility to myopia (S9 Table, Fig 4A). Gene ontology analysis revealed that these 714 genes were associated with 24 biological processes, 24 cellular components, and 14 molecular functions (S10 Table). Figure 4B shows the top 15 biological processes for the overlapping genes. Interestingly, the majority of these biological processes were suppressed in animals with high susceptibility to myopia (lower panel) and were activated in animals with negative baseline refractive errors (upper panel). A similar trend was observed when we compared canonical signaling pathways affected by the overlapping genes (S11 Table, Fig 4C). Signaling pathways, which were activated in mice with highly negative baseline refractive errors, were suppressed in mice with high susceptibility to myopia, and vice versa. The top pathways associated with both baseline refractive development and susceptibility to myopia were EIF2 signaling, protein kinase A signaling, regulation of eIF4 and p70S6K signaling, mTOR pathway, AMPK signaling, HIPPO pathway, axonal guidance signaling, synaptic long-term depression, dopamine-DARPP32

feedback signaling, and RAR signaling pathway. Figure 5 shows a summary of all signaling pathways correlated with baseline refractive eye development and susceptibility to myopia. As well as the pathways listed above, an additional 59 pathways were also implicated in both baseline refractive development and susceptibility to myopia, including synaptic long-term potentiation, CREB signaling in neurons, NRF2-mediated oxidative stress response, melatonin signaling, relaxin signaling, β-adrenergic signaling, sumoylation pathway, PTEN signaling, ephrin receptor signaling, eNOS signaling, opioid signaling pathway, and α-adrenergic signaling. Conversely, Tec kinase signaling, regulation of oleate biosynthesis, regulation of CDP-diacylglycerol biosynthesis, regulation of phosphatidylglycerol biosynthesis, regulation of Valine and Leucine degradation, dopamine receptor signaling, somatostatin receptor 2 signaling, nNOS signaling, and neurotrophin/TRK signaling were associated with baseline refractive development but not susceptibility to myopia. Super-pathway of geranylgeranyldiphosphate biosynthesis, regulation of angiogenesis by TSP1, regulation of choline biosynthesis, and chondroitin sulfate biosynthesis were associated with susceptibility to myopia but not baseline refractive error. Thus, these data suggest that baseline refractive errors and susceptibility to myopia are regulated by genetic networks with considerable overlap; however, the two genetic networks each have substantial unique components, which may independently regulate either baseline refractive development or susceptibility to environmentally induced myopia.

Many genes regulating baseline refractive eye development or susceptibility to myopia in mice are localized within chromosomal loci linked to human myopia

Genes comprising genetic networks underlying important developmental and physiological processes often harbor mutations causing human diseases. Therefore, to identify genes associated

with susceptibility to myopia in humans, we analyzed the overlap between the genes that we found to be associated with either baseline refractive development or susceptibility to myopia in mice and genes located within human quantitative trait loci (QTLs) linked to myopia (S12 Table, Fig 6, 7 and 8). We found that 90 genes whose expression correlated with baseline refractive errors, 51 genes whose expression correlated with susceptibility to myopia, and 23 genes whose expression correlated with both baseline refractive errors and susceptibility to myopia in mice were localized within human QTLs linked to myopia (S13, S14, and S15 Tables, Fig 6). GeneOverlap analysis (Fig 6) revealed that the overlaps for the genes involved in baseline refractive development and genes involved in the regulation of susceptibility to myopia were highly significant (OR = 2.75, $P = 3.3 \times 10^{-18}$; OR = 2.03, $P = 1.2 \times 10^{-07}$; respectively). The overlap between the genes located within human QTLs and genes associated with both baseline refractive development and susceptibility to myopia in mice was weaker (OR = 1.62, $P = 0.022$); however, overall, these data suggest a functional association between genes associated with refractive eye development in mice and genes causing myopia in humans. GeneOverlap analysis revealed that a total of 164 mouse genes were located within 109 human QTLs, producing 1.5 candidate genes per QTL (S16 Table, Fig 7 and 8).

We next analyzed biological processes linked to the genes associated with refractive development in mice and localized within human myopia QTLs (S17 and S18 Tables, Fig 9). Surprisingly, we found that although several biological processes, such as cell growth and proliferation, circadian regulation of gene expression, and regulation of neuron differentiation, were implicated in both baseline refractive development and regulation of susceptibility to myopia, many biological processes underlying baseline refractive development and susceptibility to myopia appeared to be different. Our data on the genes associated with baseline refractive

development in mice and localized in human QTLs implicate several unique processes, including camera-type eye development, regulation of ion/calcium transport, regulation of membrane polarization during action potential and long-term synaptic potentiation, nitric oxide signaling, ephrin receptor signaling, glucocorticoid receptor signaling, regulation of glutamate secretion, and regulation of JAK-STAT and MAPK signaling cascades (S17 Table, Fig 9A). Conversely, the genes associated with susceptibility to myopia in mice and localized in human QTLs highlighted several different processes, including regulation of cell shape and cell migration, dorsal/ventral pattern formation, vasculature morphogenesis, photoreceptor cell function and development, cellular response to DNA damage, and small-GTPase-mediated signal transduction (S18 Table, Fig 9B). Collectively, these data suggest that there is a significant functional overlap between genes we found to be correlated with refractive eye development in mice and genes causing myopia in humans. Moreover, our data suggest that development of refractive errors in humans is associated with genes that, in mice, regulate both baseline refractive development and susceptibility to refractive changes induced by the visual environment.

Gene-based genome-wide association analysis of mouse genes identifies novel gene candidates for human myopia

To build on the significant overlap observed above between genes associated with refractive eye development in mice and human myopia QTLs, we examined whether the mouse genes whose expression level correlated with refractive error or myopia susceptibility were enriched for genetic variants associated with refractive error in humans. Human genes enriched for variants associated with refractive error were identified with MAGMA (Multi-marker Analysis of GenoMic Annotation), using single-marker summary statistics from a genome-wide association study

(GWAS) for refractive error and age-of-onset-of-spectacle-wear reported by the CREAM Consortium (N=160,420 participants; [54]) or a GWAS for refractive error by the UK Biobank Eye & Vision Consortium (N= 88,005 participants; [66]) as input. Flanking regions of 200 kb upstream and downstream of transcription start and stop sites were included, in order to capture regulatory variants influencing the expression of nearby genes.

Of the 2,302 genes associated with baseline refractive development in mice for which there were human homologs, 277 genes in the CREAM dataset were associated with refractive error in humans ($FDR < 0.05$), with 86 genes surviving Bonferroni correction ($P_{Bonferroni} < 0.05$) (S19 Table). Sixty-seven of these genes (including 43 genes with $P_{Bonferroni} < 0.05$) were localized within previously identified human QTLs (Fig 7 and 8), while 210 of the 277 genes (including 43 genes with $P_{Bonferroni} < 0.05$) have not previously been implicated in the development of refractive errors in the human population (S19 Table). When the above analysis was repeated using the (independent) UK Biobank dataset, 560 genes were associated with refractive error ($FDR < 0.05$), including 156 genes with genome-wide significance ($P_{Bonferroni} < 0.05$) (S20 Table). 488 of the 560 genes (including 104 genes with $P_{Bonferroni} < 0.05$) have not previously been implicated in the development of refractive errors in humans (S20 Table). Importantly, 190 genes associated with baseline refractive development in mice were replicated in both the CREAM and UK Biobank cohorts, including 69 genes which achieved genome-wide significance ($P_{Bonferroni} < 0.05$) (S23 Table).

Of the 1,917 genes associated with the regulation of susceptibility to myopia in mice, gene-based analysis using the CREAM dataset identified 223 genes associated with refractive error in humans ($FDR < 0.05$), including 72 genes at genome-wide significance ($P_{Bonferroni} < 0.05$) (S21 Table). Forty-six of these genes (including 33 genes with $P_{Bonferroni} < 0.05$) were localized within

previously identified human QTLs (Fig 7 and 8), whereas 177 of the 223 genes (including 39 genes with $P_{Bonferroni} < 0.05$) have not previously been implicated in the development of refractive errors in humans (S21 Table). MAGMA analysis of the 1,917 genes using the UK Biobank dataset revealed that 465 genes were associated with refractive error ($FDR < 0.05$), including 119 genes that withstood Bonferroni correction ($P_{Bonferroni} < 0.05$) (S22 Table). Forty-nine of these genes (including 35 genes with $P_{Bonferroni} < 0.05$) were localize within known human myopia QTLs (Fig 7 and 8), whereas 416 of the 465 genes (including 84 genes with $P_{Bonferroni} < 0.05$) were not previously known to be associated with the development of refractive errors in the human population (S22 Table). One hundred and fifty-two genes involved in the regulation of susceptibility to myopia in mice were found to be linked to the development of refractive errors in both CREAM and UK Biobank cohorts, including 53 genes which reached genome-wide significance ($P_{Bonferroni} < 0.05$) in both samples (S24 Table).

Analysis of the biological processes associated with the above genes linked to either baseline refractive development or regulation of susceptibility to myopia in humans (S25 and S26 Tables, Fig 10A and 11A) revealed processes primarily related to calcium-mediated cell adhesion, synapse assembly, synaptic transmission, protein translation, small GTPase-mediated signal transduction, and GABA receptor signaling. Several canonical signaling pathways were also identified, including EIF2 and mTOR signaling, eIF4 and p70S6K signaling, epithelial adherence junction signaling, sumoylation pathway, and regulation of cellular mechanics by calpain protease, among others (S27 and S28 Tables, Fig 10B and 11B).

However, there were also substantial differences between the two sets of human genes identified using either the mouse baseline refractive error or the mouse myopia susceptibility gene sets. The mouse baseline refractive error-derived human gene set was associated with nervous

system development, post-embryonic camera-type eye development, retinal cone development, neuron migration, dendrite morphogenesis, regulation of glutamate metabolism, extracellular matrix organization, and beta-amyloid formation (S25 Table, Fig 10A). This gene set was associated with several canonical pathways distinct from those identified using the mouse susceptibility to myopia-derived human gene set. These pathways included integrin signaling, semaphorin signaling in neurons, glucocorticoid receptor signaling, phospholipase C signaling, synaptic long term potentiation, ephrin receptor signaling, nNOS signaling in neurons, and estrogen receptor signaling (S27 and S28 Tables, Fig 10B and 11B).

The mouse susceptibility to myopia-derived human gene set, on the other hand, was associated with biological processes related to developmental growth, neuron fate commitment, regulation of mesenchymal cell proliferation, potassium ion transmembrane transport, protein transport, response to estradiol and cholesterol, as well as cellular response to hypoxia (S26 Table, Fig 11A). Analysis of canonical pathways suggested that pathways associated with TGF-β signaling, PPARα/RXRα activation, PTEN signaling, regulation of the epithelial-mesenchymal transition, STAT3 signaling, regulation of stem cell pluripotency, VEGF and IGF-1 signaling, NRF2-mediated oxidative stress response, and PI3K/AKT signaling, among others, were involved in the regulation of susceptibility to myopia (S28 Table, Fig 11B).

Discussion

Human population studies and studies in animal models strongly suggest that both environmental and genetic factors play important roles in refractive eye development. Numerous linkage and genome-wide association studies in humans identified over 270 chromosomal loci linked to the development of myopia in humans; however, very little is known how genetic variation causing

myopia affects gene expression and how changes in gene expression associated with differences in genetic backgrounds affect refractive eye development and susceptibility to myopia.

Our data suggest that differences in genetic backgrounds play a very important role in refractive eye development and regulation of susceptibility to myopia. Moreover, we found that variations in genetic background produce a continuous distribution of refractive errors and susceptibilities to myopia in a mouse population characteristic of quantitative traits. Genetic variations in different mouse strains also produce unique patterns of gene expression, which strongly correlate with either baseline refractive errors or susceptibility to induced myopia. Surprisingly, we found that refractive eye development and susceptibility to myopia are controlled by largely distinct sets of genes, which suggests that signaling pathways that regulate the trajectory of refractive eye development towards emmetropia, myopia, or hyperopia might be different from the pathways that modulate the impact of optical defocus and other environmental factors on refractive development. However, expression of 714 genes correlated with both baseline refractive errors and susceptibility to myopia, suggesting that at least these genes can control both the pathways regulating the trajectory of refractive development and the impact of visual input on it.

Genes that influenced either baseline refractive development or susceptibility to myopia affected a long list of biological and molecular functions; however, most noteworthy is the finding that over 84 canonical signaling pathways were involved in both baseline refractive development and regulation of susceptibility to myopia. Interestingly, the majority of these pathways were suppressed in animals with high susceptibility to myopia and activated in animals with negative baseline refractive errors. The exceptions from this rule were sumoylation, HIPPO, and PTEN signaling pathways, which we found to be activated in animals with high susceptibility to myopia and suppressed in animals with negative baseline refractive errors. The observation that the same

pathways were effected in the opposite directions in animals with high susceptibility to myopia and animals with highly negative baseline refractive errors may be explained by the role of optical defocus in the development of myopia. Considering that mice are housed in small cages and the exposure to distant vision is limited, animals with hyperopic refractive errors would be exposed to high levels of hyperopic optical defocus (which was shown to cause myopia) compared to the animals with negative refractive errors; thus explaining why signaling pathways are effected in the same direction in animals with high susceptibility to myopia and animals with hyperopic baseline refractive errors.

Remarkably, we also found that many genes whose expression correlated with either baseline refractive errors or susceptibility to myopia in mice were localized in the known human QTLs linked to myopia. The majority of these genes (90 genes) were exclusively involved in baseline refractive eye development, 51 genes were linked to the regulation of susceptibility to myopia, and 23 genes affected both baseline refractive development and susceptibility to myopia.

Gene-based genome-wide association analysis of the genes we found in mice against CREAM and UK Biobank human samples revealed that 647 genes whose expression correlated with baseline refractive errors in mice were also associated with refractive errors in humans, including 173 genes that withstood Bonferroni correction. Using gene-based analysis, we also found that a total of 536 genes whose expression correlated with susceptibility to myopia were associated with refractive errors in humans, including 138 genes which exhibited genome-wide significance ($P_{Bonferroni} < 0.05$). One hundred and ninety-eight of these genes were involved in both baseline refractive development and regulation of susceptibility to myopia, including 34 genes which withstood Bonferroni correction. Although many of these genes were previously implicated in the development of human myopia, 572 genes (92 genes with $P_{Bonferroni} < 0.05$) whose expression

correlated with baseline refractive development and 486 genes (79 genes with $P_{Bonferroni} < 0.05$) whose expression correlated with susceptibility to myopia were linked to human myopia for the first time, including 211 genes (54 genes with $P_{Bonferroni} < 0.05$) whose expression correlated with both baseline refractive development and susceptibility to myopia.

Genes that we found to be involved in refractive error development in mice and humans affect a multitude of biological functions in the retina; however, many biological functions underlying refractive development appear to be highly conserved across species. These include camera-type eye development and post-embryonic eye morphogenesis, ephrin receptor signaling, glucocorticoid receptor signaling, regulation of circadian rhythms and circadian regulation of gene expression, glutamate signaling, regulation of neurogenesis and dendrite morphogenesis, regulation of nitric oxide biosynthesis, regulation of long-term synaptic potentiation, synapse assembly and chemical synapse transmission, calcium-dependent signaling, regulation of translation, small GTPase mediated signal transduction, photoreceptor function and development, cell-cell adhesion, regulation of beta-amyloid formation, regulation of mesenchymal cell proliferation, cellular response to hypoxia. We also found that many retinal signaling pathways involved in refractive development in mice are also subjected to genetic variation causing myopia in humans. These include EIF2 signaling, regulation of eIF4 and p70S6K signaling, mTOR signaling, integrin signaling, semaphorin signaling in neurons, protein kinase A signaling, clathrin-mediated endocytosis signaling, epithelial adherens junction signaling, synaptic long term potentiation, ephrin receptor signaling, nNOS and eNOS signaling, estrogen receptor signaling, PPARα/RXRα activation, signaling by Rho family GTPases, Wnt/Ca+ pathway, dopamine-DARPP32 feedback signaling, PTEN signaling, IGF-1 signaling, insulin receptor signaling, NF-κB signaling, RAR signaling, amyloid processing, among other pathways.

Interestingly, 27 genes that we found to be associated with refractive error development in mice were also among the genes differentially expressed in the retina of green monkeys with form-deprivation-induced myopia [39], and 233 genes were among the genes differentially expressed in the retina of marmosets exposed to positive and negative optical defocus [67]. There was also a 47-gene overlap with the genes found by Riddell et al. to be differentially expressed in the retina of chicks exposed to optical defocus [68], while 292 genes found in mice overlapped with genes found to be differentially expressed in the retina of chicks with lens-induced myopia by Stone et al. [69]. Many of the genes that we found to be involved in refractive eye development in this study had been previously implicated in various physiological and pathological processes in the retina. For example, mutations in *TTC21B* gene, which we found to be involved in the regulation of susceptibility to myopia, were shown to cause a syndromic form of retinal dystrophy [70]. Mutations in *EFEMP1* (gene involved in baseline refractive development) were found to be associated with Malattia Leventinese retinal dystrophy characterized by the presence of RPE deposits [71]. Several studies linked a manganese transporter *SLC30A10*, which was found in this study to be involved in baseline refractive development, to parkinsonism, thus implicating this gene in the regulation of dopamine signaling [72, 73]. Ephrin receptor A10 (*EPHA10*), which we found to be involved in the regulation of susceptibility to myopia, was shown to influence cone photoreceptor morphogenesis, implicating signaling at the level of photoreceptors in refractive eye development [74]. A GTP-binding protein GNL2, involved in baseline refractive development, was demonstrated to play important role in retinal neurogenesis [75]. Finally, *AGRN* gene, found by this study to be involved in baseline refractive development, was shown to interact with EGR1 (previously implicated in refractive eye development) and regulate synaptic physiology in the retina [76, 77].

Although many pathways that we found to underlie refractive development in mice and humans in this study are novel, many of them had previously been implicated in refractive eye development and/or development of myopia in other species. Seven out of 47 pathways found to be involved in optical defocus response in chickens by Riddell et al. [62] were also found to be involved in refractive eye development in this study, including PPAR signaling, tight junction signaling, Huntington's disease signaling, cysteine metabolism, actin cytoskeleton signaling, TGF-β signaling, and Glutathione metabolism (S5, S8, S27, and S28 Tables). We replicated 12 out of 20 canonical pathways identified by Stone et al. [69] in chickens with lens-induced myopia, including glutamate receptor signaling, β-adrenergic signaling, synaptic long term depression, synaptic long term potentiation, amyotrophic lateral sclerosis signaling, CREB signaling in neurons, relaxin signaling, purine metabolism, CDK5 signaling, protein kinase A signaling, hypoxia signaling, and tight junction signaling (S5, S8, S27, and S28 Tables). We also found that 35 out of 75 pathways that we recently found to be involved in the development of hyperopia and myopia in marmosets [67] were also among the pathways which we found to be involved in refractive eye development in this study, including Ephrin Receptor Signaling, β-adrenergic Signaling, Protein Kinase A Signaling, Relaxin Signaling, Androgen Signaling, Dopamine-DARPP32 Feedback Signaling, nNOS Signaling, RAN Signaling, HIPPO signaling, Wnt/Ca+ pathway, PTEN Signaling, Synaptic Long Term Potentiation, Gap Junction Signaling, Regulation of eIF4 and p70S6K Signaling, mTOR Signaling, Glucocorticoid Receptor Signaling, α-Adrenergic Signaling, and Epithelial Adherens Junction Signaling, among others (S5, S8, S27, and S28 Tables). An important role of amyloid signaling pathway, which we found to be involved in the regulation of susceptibility to myopia (S8 Table), is an agreement with our recent finding that a component of the amyloid signaling pathway APLP2 regulates susceptibility to myopia in mice

and humans [37]. Our data also suggest that the phototransduction pathway is involved in refractive eye development (S5 Table), in agreement with a recent GWAS study [54] and recent marmoset data [67].

In summary, we have identified 2,302 genes which are involved in baseline refractive eye development and 1,917 genes which regulate susceptibility to myopia in mice. Our data suggest that at least 985 of these genes are subjected to genetic variation in the human population and are involved in refractive error development in humans. Eight hundred forty-seven of these genes were implicated in the development of human myopia for the first time. A large number of common genes and canonical pathways that we found to be involved in the regulation of refractive eye development in mice, chickens and humans suggests strong evolutionary conservation of the signaling pathways underlying refractive error development. It appears that the number of genes involved in the regulation of refractive eye development may be as high as 3,505 in the retina alone, suggesting that refractive eye development maybe regulated by hundreds to thousands of genes across ocular tissues. Interestingly, in spite of significant overlap between genes that control baseline refractive development and genes regulating susceptibility to myopia, these two processes appear to be controlled by largely distinct sets of genes. The genes that we found to be involved in refractive eye development control, however, a well-defined set of retinal signaling pathways that we begin to consistently find to be involved in refractive eye development across different species. This provides a solid framework for future studies and for the development of anti-myopia drugs.

Materials and Methods

Ethics statement

Mice were obtained from the Jackson Laboratory (Bar Harbor, ME) and were maintained as an in-house breeding colony. All procedures adhered to the Association for Research in Vision and Ophthalmology (ARVO) statement on the use of animals in ophthalmic and vision research and were approved by the Columbia University Institutional Animal Care and Use Committee. Animals were anesthetized via intraperitoneal injection of ketamine (90 mg/kg) and xylazine (10 mg/kg) and were euthanized using CO_2 followed by cervical dislocation.

All human studies were approved by the relevant institutional review boards and/or medical ethics committees and conducted according to the Declaration of Helsinki. All CREAM participants provided written informed consent. The UK Biobank received ethical approval from the National Health Service National Research Ethics Service (reference 11/NW/0382).

Analysis of refractive state of the eyes in mice

To examine the effect of genetic background on the refractive state of the eye in mice, we analyzed baseline refractive errors in the eight strains of mice comprising Collaborative Cross. The refractive state of both left and right eyes was determined on alert animals at P40 using an automated eccentric infrared photorefractor as previously described [65, 78]. The animal to be refracted was immobilized using a restraining platform, and each eye was refracted along the optical axis in dim room light (< 1 lux), 20-30 min. after instilling 1% tropicamide ophthalmic solution (Alcon Laboratories) to ensure mydriasis and cycloplegia. Five independent measurement series (~300-600 measurements each) were taken for each eye. The measurements were automatically acquired by the photorefractor every 16 msec. Each successful measurement series (i.e., Purkinje image in the center of the pupil and stable refractive error for at least 5 sec.) was marked by a green LED flash, which was registered by the photorefractor software. Sixty

individual measurements from each series, immediately preceding the green LED flash, were combined, and a total of 300 measurements (60 measurements x 5 series = 300 measurements) were collected for each eye. Data for the left and right eyes were combine (600 measurements total) to calculate mean refractive error and standard deviation for each animal.

Analysis of form-deprivation myopia in mice

To examine the effect of genetic background on susceptibility to environmentally induced myopia in mice, we analyzed the extent of myopia induced by the diffuser-imposed retinal image degradation (visual form deprivation) in the eight strains of mice comprising Collaborative Cross. Visual input was degraded in one of the eyes by applying plastic diffusers, and refractive development of the treated eye was compared to that of the contralateral eye, which was not treated with a diffuser, as previously described [79, 80]. Diffusers represented low-pass optical filters, which degraded the image projected onto the retina by removing high spatial frequency details. Frosted hemispherical plastic diffusers were hand-made from zero power rigid contact lenses made from OP3 plastic (diameter = 7.0 mm, base curve = 7.0 mm; Lens.com). Lenses were frosted using a fine sandpaper and inserted into a 3D-printed plastic frames (Proto Labs). On the first day of the experiment (P24), animals were anesthetized via intraperitoneal injection of ketamine and xylazine, and frames with diffusers were attached to the skin surrounding the right eye with six stitches using size 5-0 ETHILON™ microsurgical sutures (Ethicon) and reinforced with Vetbond™ glue (3M Animal Care Products) (the left eye served as a control). Toenails were covered with adhesive tape to prevent mice from removing the diffusers. Animals recovered on a warming pad and were then housed under low-intensity constant light in transparent plastic cages for the duration of the experiment as previously described [79, 80]. Following 21 days of visual

form deprivation (from P24 through P45), diffusers were removed and refractive status of both treated and control eyes was assessed using an automated eccentric infrared photorefractor as previously described [65, 78]. The interocular difference in refraction between the treated and contralateral control eye served as an indication of the extent of induced myopia.

RNA extraction and RNA-seq

Animals were euthanized following an IACUC-approved protocol. Eyes were enucleated, the retinae were dissected from the enucleated eyes and the choroid/RPE removed. The retinae were washed in RNAlater (Thermo Fisher Scientific) for 5 min., frozen in liquid nitrogen, and stored at -80°C until processed for this study. To isolate RNA, tissue samples were homogenized at 4°C in a lysis buffer using Bead Ruptor 24 tissue homogenizer (Omni). Total RNA was extracted from each tissue sample using miRNAeasy mini kit (QIAGEN) following the manufacturer's protocol. The integrity of RNA was confirmed by analyzing 260/280 nm ratios ($Ratio_{260/280}$ = 2.11-2.13) on a Nanodrop (Thermo Scientific) and the RNA Integrity Number (RIN = 9.0-10.0) using Agilent Bioanalyzer. Illumina sequencing libraries were constructed from 1 μg of total RNA using the TruSeq Stranded Total RNA LT kit with the Ribo-Zero Gold ribosomal RNA depletion module (Illumina). Each library contained a specific index (barcode) and were pooled at equal concentrations using the randomized complete block (RCB) experimental design before sequencing on Illumina HiSeq 2500 sequencing system. The number of libraries per multiplexed sample was adjusted to ensure sequencing depth of ~70 million reads per library (paired-end, 2 x 100 nucleotides). The actual sequencing depth was 76,773,554 ± 7,832,271 with read quality score 34.5 ± 0.4.

Post-sequencing RNA-seq data validation and analysis

The FASTQ raw data files generated by the Illumina sequencing system were imported into Partek Flow software package (version 7.0.18.1210, Partek), libraries were separated based on their barcodes, adapters were trimmed and remaining sequences were subjected to pre-alignment quality control using Partek Flow pre-alignment QA/QC module. After the assessment of various quality metrics, bases with the quality score < 34 were removed (≤ 5 bases) from each end. Sequencing reads were then mapped to the mouse reference genome Genome Reference Consortium Mouse Build 38 (GRCm38/mm10, NCBI) using the STAR aligner (version 2.5.2b) resulting in 95.0 ± 0.4% mapped reads per library, which covered 35.4 ± 1.0% of the genome. Aligned reads were quantified to transcriptome using Partek E/M annotation model and the NCBI's RefSeq Transcripts 80 annotation file to determine read counts per gene/genomic region. The generated read counts were normalized by the total read count and subjected to the analysis of variance (ANOVA) to detect genes whose expression correlates with either refractive error or susceptibility to myopia. Differentially expressed transcripts were identified using a P-value threshold of 0.05 adjusted for genome-wide statistical significance using Storey's q-value algorithm [81]. To identify sets of genes with coordinate expression, differentially expressed transcripts were clustered using Partek Flow hierarchical clustering module using average linkage for the cluster distance metric and Euclidean distance metric to determine the distance between data points. Each RNA-seq sample was analyzed as a biological replicate, thus, resulting in three biological replicates per strain.

Gene ontology analysis and identification of canonical signaling pathways

To identify biological functions (gene ontology categories), which were significantly affected by the genes whose expression correlated with either baseline refractive errors or susceptibility to myopia, we used the database for annotation, visualization and integrated discovery (DAVID) version 6.8 [82] and GOplot R package [83]. DAVID uses a powerful gene-enrichment algorithm and DAVID Gene Concept database to identify biological functions (gene ontology categories) affected by differential genes, while GOplot integrates gene ontology information with gene expression information and predicts the effect of gene expression changes on biological processes. DAVID uses a modified Fisher's exact test (EASE score) with a P-value threshold of 0.05 to estimate statistical significance of enrichment for specific gene ontology categories. IPA Pathways Activity Analysis module (QIAGEN) was used to identify canonical pathways effected by the genes involved in baseline refractive eye development or regulating susceptibility to myopia, and predict the effect of gene expression changes in different strains on specific pathways. The activation z-score was employed in the IPA Pathways Activity Analysis module to predict activation or suppression of the canonical pathways. The z-score algorithm is designed to reduce the chance that random data will generate significant predictions. The z-score provides an estimate of statistical quantity of change for each pathway found to be statistically significantly affected by the changes in gene expression. The significance values for the canonical pathways were calculated by the right-tailed Fisher's exact test. The significance indicates the probability of association of molecules from a dataset with the canonical pathway by random chance alone. Pathways Activity Analysis module determines if canonical pathways, including functional end-

points, are activated or suppressed based on the gene expression data in a dataset. Once statistically significant canonical pathways were identified, we subjected the datasets to the Core Functional Analysis in IPA to compare the pathways and identify key similarities and differences in the canonical pathways underlying baseline refractive development and susceptibility to myopia.

Identification of candidate genes for human myopia within known myopia QTLs

To identify candidate genes for myopia in the QTLs previously found to be linked to human myopia, we compared the genes that we found to be involved in refractive eye development in mice with a list of genes located within human myopia QTLs. We first compiled a list of all SNPs or markers exhibiting statistically significant association with myopia in the human linkage or GWAS studies. LDlink's LDmatrix tool (National Cancer Institute) was used to identify SNPs in linkage disequilibrium and identify overlapping chromosomal loci. We then used UCSC Table Browser to extract all genes located within critical chromosomal regions identified by the human linkage studies or within 200 kb (±200 kb) of the SNPs found by GWAS. The list of genes located within human QTLs was compared with the list of genes that we found to be associated with either baseline refractive errors or susceptibility to myopia in mice using Partek Genomics Suite (Partek). The statistical significance of the overlaps was estimated using probabilities associated with the hypergeometric distribution using Bioconductor software package GeneOverlap version 1.14.0 and associated functions.

Identification of genes associated with refractive error in the human population using gene-based genome-wide association analysis

To identify genes associated with the development of refractive errors in humans among the genes whose expression correlated with refractive eye development in mice, human homologs of candidate mouse genes were examined for association with refractive error in the international genome-wide association study (GWAS) of refractive error carried out by the Consortium for Refractive Error and Myopia (CREAM) [54] and the UK Biobank Eye and Vision consortium sample [66] using the Multi-marker Analysis of GenoMic Annotation (MAGMA) [84]. Human homologs of candidate mouse genes were obtained from Ensembl BioMart and were mapped according to gene definitions in the NCBI Entrez Gene database. Genes were defined according to NCBI build 37 (hg19/GRCh37) coordinates with 200kb flanking regions appended to the transcription start/stop sites. LD patterns were estimated by MAGMA using the 1000 Genomes Phase 1, version 3 European ancestry reference panel. As summary statistics were used as input, MAGMA gene-based analysis was performed using the default "snp-wise=mean" model.

The CREAM sample included 148,485 individuals of European ancestry from 28 cohorts and 11,935 individuals of Asian ancestry from eight studies. All participants included in this analysis from CREAM were 25 years of age or older.

UK Biobank is a large prospective study following the health and wellbeing of approximately 500,000 UK residents aged between 40 and 69 years-old at the baseline recruitment visit (during the period 2006–2010). 130,521 participants had non-cycloplegic autorefraction performed for at least one eye using the Tomey RC 5000 autorefractor-keratometer (Tomey Corp., Nagoya, Japan), with up to ten measurements taken for each eye. After the exclusion of unreliable readings, 130,459 participants had measures for refractive astigmatism and spherical equivalent refractive error.

Participants with conditions that might alter refraction, such as cataract surgery, laser refractive procedures, retinal detachment surgery, keratoconus, or ocular or systemic syndromes were excluded from the analyses. Refractive error was represented by measurements of refraction and analyzed as spherical equivalent (SphE = spherical refractive error +1/2-cylinder refractive error).

Acknowledgements

We are grateful to all the individuals who took part in the CREAM and UK Biobank studies, the personnel who recruited them, interviewers, computer and laboratory technicians, clerical workers, research scientists, volunteers, managers, receptionists and nurses. This research has been conducted using the UK Biobank Resource (application #17351). Special thanks to Jeremy Guggenheim who provided valuable feedback on an early version of the manuscript.

References

1. Pararajasegaram R. VISION 2020-the right to sight: from strategies to action. Am J Ophthalmol. 1999;128(3):359-360. PubMed PMID: 10511033.
2. Kempen JH, Mitchell P, Lee KE, Tielsch JM, Broman AT, Taylor HR, et al. The prevalence of refractive errors among adults in the United States, Western Europe, and Australia. Arch Ophthalmol. 2004;122(4):495-505. doi: 10.1001/archopht.122.4.495. PubMed PMID: 15078666.
3. Javitt JC, Chiang YP. The socioeconomic aspects of laser refractive surgery. Arch Ophthalmol. 1994;112(12):1526-1530. PubMed PMID: 7993206.
4. Vitale S, Sperduto RD, Ferris FL, 3rd. Increased prevalence of myopia in the United States between 1971-1972 and 1999-2004. Arch Ophthalmol. 2009;127(12):1632-1639. doi: 10.1001/archophthalmol.2009.303. PubMed PMID: 20008719.
5. Holden BA, Fricke TR, Wilson DA, Jong M, Naidoo KS, Sankaridurg P, et al. Global Prevalence of Myopia and High Myopia and Temporal Trends from 2000 through 2050. Ophthalmology. 2016;123(5):1036-1042. doi: 10.1016/j.ophtha.2016.01.006. PubMed PMID: 26875007.

6. Lin LL, Shih YF, Hsiao CK, Chen CJ. Prevalence of myopia in Taiwanese schoolchildren: 1983 to 2000. Ann Acad Med Singapore. 2004;33(1):27-33. Epub 2004/03/11. PubMed PMID: 15008558.
7. Lam CS, Goldschmidt E, Edwards MH. Prevalence of myopia in local and international schools in Hong Kong. Optom Vis Sci. 2004;81(5):317-322. Epub 2004/06/08. doi: 00006324-200405000-00009 [pii]. PubMed PMID: 15181356.
8. Alexander LJ. Primary care of the posterior segment. 2 ed. Connecticut: Appleton & Lange; 1994.
9. Saw SM, Gazzard G, Shih-Yen EC, Chua WH. Myopia and associated pathological complications. Ophthalmic Physiol Opt. 2005;25(5):381-391. Epub 2005/08/17. doi: OPO298 [pii] 10.1111/j.1475-1313.2005.00298.x. PubMed PMID: 16101943.
10. Flitcroft DI. The complex interactions of retinal, optical and environmental factors in myopia aetiology. Prog Retin Eye Res. 2012;31(6):622-660. doi: 10.1016/j.preteyeres.2012.06.004. PubMed PMID: 22772022.
11. Hurst J, Johnson D, Law C, Schweitzer K, Sharma S. Value of subjective visual reduction in patients with acute-onset floaters and/or flashes. Can J Ophthalmol. 2015;50(4):265-268. Epub 2015/08/11. doi: 10.1016/j.jcjo.2015.06.001. PubMed PMID: 26257218.
12. Shunmugam M, Ang GS, Lois N. Giant retinal tears. Surv Ophthalmol. 2014;59(2):192-216. Epub 2013/10/22. doi: 10.1016/j.survophthal.2013.03.006. PubMed PMID: 24138895.
13. Rumelt S, Sarrazin L, Averbukh E, Halpert M, Hemo I. Paediatric vs adult retinal detachment. Eye (Lond). 2007;21(12):1473-1478. Epub 2006/08/01. doi: 10.1038/sj.eye.6702511. PubMed PMID: 16878114.
14. Brasil OF, Brasil MV, Japiassu RM, Biancardi AL, Souza DD, Oliveira RC, et al. [Fundus changes evaluation in degenerative myopia]. Arquivos brasileiros de oftalmologia. 2006;69(2):203-206. Epub 2006/05/16. doi: /S0004-27492006000200013. PubMed PMID: 16699671.
15. Ndiaye PA, Koffane RR, Wade A, Ndiaye CS, Gomez JC, Ndiaye MR. [Frequency of retinal changes in myopia in a black population]. J Fr Ophtalmol. 2001;24(9):927-929. Epub 2002/03/27. PubMed PMID: 11912835.
16. Bonnet M. [Myopia and rhegmatogenous retinal detachment]. Rev Prat. 1993;43(14):1779-1783. Epub 1993/09/15. PubMed PMID: 8310217.
17. Pierro L, Camesasca FI, Mischi M, Brancato R. Peripheral retinal changes and axial myopia. Retina. 1992;12(1):12-17. Epub 1992/01/01. PubMed PMID: 1565864.
18. Grossniklaus HE, Green WR. Pathologic findings in pathologic myopia. Retina. 1992;12(2):127-133. Epub 1992/01/01. PubMed PMID: 1439243.
19. Burton TC. The influence of refractive error and lattice degeneration on the incidence of retinal detachment. Trans Am Ophthalmol Soc. 1989;87:143-155; discussion 155-147. Epub 1989/01/01. PubMed PMID: 2562517; PubMed Central PMCID: PMCPMC1298542.
20. Pruett RC, Weiter JJ, Goldstein RB. Myopic cracks, angioid streaks, and traumatic tears in Bruch's membrane. Am J Ophthalmol. 1987;103(4):537-543. Epub 1987/04/15. PubMed PMID: 3565514.
21. Chaine G, Sebag J, Coscas G. The induction of retinal detachment. Trans Ophthalmol Soc U K. 1983;103 (Pt 4):480-485. Epub 1983/01/01. PubMed PMID: 6589866.
22. Menezo JL, Suarez-Reynolds R, Frances J, Vila E. Shape, number and localization of retinal tears in myopic over 8D, aphakic and traumatic cases of retinal detachment. An experience report. Ophthalmologica. 1977;175(1):10-18. Epub 1977/01/01. PubMed PMID: 904882.

23. Kanski JJ. Giant retinal tears. Am J Ophthalmol. 1975;79(5):846-852. Epub 1975/05/01. PubMed PMID: 1146947.
24. Verhoeven VJ, Wong KT, Buitendijk GH, Hofman A, Vingerling JR, Klaver CC. Visual consequences of refractive errors in the general population. Ophthalmology. 2015;122(1):101-109. doi: 10.1016/j.ophtha.2014.07.030. PubMed PMID: 25208857.
25. Qiu M, Wang SY, Singh K, Lin SC. Association between myopia and glaucoma in the United States population. Invest Ophthalmol Vis Sci. 2013;54(1):830-835. doi: 10.1167/iovs.12-11158. PubMed PMID: 23299483; PubMed Central PMCID: PMC3562121.
26. Praveen MR, Vasavada AR, Jani UD, Trivedi RH, Choudhary PK. Prevalence of cataract type in relation to axial length in subjects with high myopia and emmetropia in an Indian population. Am J Ophthalmol. 2008;145(1):176-181. doi: 10.1016/j.ajo.2007.07.043. PubMed PMID: 17936714; PubMed Central PMCID: PMC2199267.
27. Loyo-Berrios NI, Blustein JN. Primary-open glaucoma and myopia: a narrative review. WMJ : official publication of the State Medical Society of Wisconsin. 2007;106(2):85-89, 95. PubMed PMID: 17479825.
28. Pizzarello L, Abiose A, Ffytche T, Duerksen R, Thulasiraj R, Taylor H, et al. VISION 2020: The Right to Sight: a global initiative to eliminate avoidable blindness. Arch Ophthalmol. 2004;122(4):615-620. doi: 10.1001/archopht.122.4.615. PubMed PMID: 15078680.
29. Morgan IG. The biological basis of myopic refractive error. Clin Exp Optom. 2003;86(5):276-288. Epub 2003/10/16. doi: ceo865276 [pii]. PubMed PMID: 14558849.
30. Young TL. Molecular genetics of human myopia: an update. Optom Vis Sci. 2009;86(1):E8-E22. Epub 2008/12/24. doi: 10.1097/OPX.0b013e3181940655. PubMed PMID: 19104467.
31. Baird PN, Schache M, Dirani M. The GEnes in Myopia (GEM) study in understanding the aetiology of refractive errors. Prog Retin Eye Res. 2010;29(6):520-542. Epub 2010/06/26. doi: S1350-9462(10)00034-0 [pii] 10.1016/j.preteyeres.2010.05.004. PubMed PMID: 20576483.
32. Wojciechowski R. Nature and nurture: the complex genetics of myopia and refractive error. Clin Genet. 2011;79(4):301-320. Epub 2010/12/16. doi: 10.1111/j.1399-0004.2010.01592.x. PubMed PMID: 21155761; PubMed Central PMCID: PMC3058260.
33. Parssinen O, Lyyra AL. Myopia and myopic progression among schoolchildren: a three-year follow-up study. Invest Ophthalmol Vis Sci. 1993;34(9):2794-2802. Epub 1993/08/01. PubMed PMID: 8344801.
34. Goss DA. Nearwork and myopia. Lancet. 2000;356(9240):1456-1457. Epub 2000/11/18. doi: S0140-6736(00)02864-6 [pii] 10.1016/S0140-6736(00)02864-6. PubMed PMID: 11081523.
35. Hepsen IF, Evereklioglu C, Bayramlar H. The effect of reading and near-work on the development of myopia in emmetropic boys: a prospective, controlled, three-year follow-up study. Vision Res. 2001;41(19):2511-2520. Epub 2001/08/03. doi: S0042-6989(01)00135-3 [pii]. PubMed PMID: 11483181.
36. Saw SM, Chua WH, Hong CY, Wu HM, Chan WY, Chia KS, et al. Nearwork in early-onset myopia. Invest Ophthalmol Vis Sci. 2002;43(2):332-339. Epub 2002/01/31. PubMed PMID: 11818374.
37. Tkatchenko AV, Tkatchenko TV, Guggenheim JA, Verhoeven VJ, Hysi PG, Wojciechowski R, et al. APLP2 Regulates Refractive Error and Myopia Development in Mice and Humans. PLoS Genet. 2015;11(8):e1005432. doi: 10.1371/journal.pgen.1005432. PubMed PMID: 26313004.

38. Troilo D, Li T, Glasser A, Howland HC. Differences in eye growth and the response to visual deprivation in different strains of chicken. Vision Res. 1995;35(9):1211-1216. Epub 1995/05/01. doi: 0042-6989(94)00230-J [pii]. PubMed PMID: 7610582.
39. Tkatchenko AV, Walsh PA, Tkatchenko TV, Gustincich S, Raviola E. Form deprivation modulates retinal neurogenesis in primate experimental myopia. Proc Natl Acad Sci U S A. 2006;103(12):4681-4686. Epub 2006/03/16. doi: 0600589103 [pii] 10.1073/pnas.0600589103. PubMed PMID: 16537371; PubMed Central PMCID: PMC1400590.
40. Schaeffel F, Burkhardt E, Howland HC, Williams RW. Measurement of refractive state and deprivation myopia in two strains of mice. Optom Vis Sci. 2004;81(2):99-110. Epub 2004/05/07. doi: 00006324-200402000-00008 [pii]. PubMed PMID: 15127929.
41. Chen YP, Hocking PM, Wang L, Povazay B, Prashar A, To CH, et al. Selective breeding for susceptibility to myopia reveals a gene-environment interaction. Invest Ophthalmol Vis Sci. 2011;52(7):4003-4011. Epub 2011/03/26. doi: 10.1167/iovs.10-7044. PubMed PMID: 21436268.
42. Zhou G, Williams RW. Mouse models for the analysis of myopia: an analysis of variation in eye size of adult mice. Optom Vis Sci. 1999;76(6):408-418. Epub 1999/07/23. PubMed PMID: 10416936.
43. Puk O, Dalke C, Favor J, de Angelis MH, Graw J. Variations of eye size parameters among different strains of mice. Mamm Genome. 2006;17(8):851-857. Epub 2006/08/10. doi: 10.1007/s00335-006-0019-5. PubMed PMID: 16897341.
44. Wong AA, Brown RE. Visual detection, pattern discrimination and visual acuity in 14 strains of mice. Genes Brain Behav. 2006;5(5):389-403. Epub 2006/08/02. doi: GBB173 [pii] 10.1111/j.1601-183X.2005.00173.x. PubMed PMID: 16879633.
45. Peet JA, Cotch MF, Wojciechowski R, Bailey-Wilson JE, Stambolian D. Heritability and familial aggregation of refractive error in the Old Order Amish. Invest Ophthalmol Vis Sci. 2007;48(9):4002-4006. Epub 2007/08/29. doi: 48/9/4002 [pii] 10.1167/iovs.06-1388. PubMed PMID: 17724179; PubMed Central PMCID: PMC1995233.
46. Lyhne N, Sjolie AK, Kyvik KO, Green A. The importance of genes and environment for ocular refraction and its determiners: a population based study among 20-45 year old twins. Br J Ophthalmol. 2001;85(12):1470-1476. Epub 2001/12/06. PubMed PMID: 11734523; PubMed Central PMCID: PMC1723806.
47. Hammond CJ, Snieder H, Gilbert CE, Spector TD. Genes and environment in refractive error: the twin eye study. Invest Ophthalmol Vis Sci. 2001;42(6):1232-1236. Epub 2001/05/01. PubMed PMID: 11328732.
48. Teikari JM, Kaprio J, Koskenvuo MK, Vannas A. Heritability estimate for refractive errors--a population-based sample of adult twins. Genet Epidemiol. 1988;5(3):171-181. Epub 1988/01/01. doi: 10.1002/gepi.1370050304. PubMed PMID: 3049225.
49. Dirani M, Chamberlain M, Shekar SN, Islam AF, Garoufalis P, Chen CY, et al. Heritability of refractive error and ocular biometrics: the Genes in Myopia (GEM) twin study. Invest Ophthalmol Vis Sci. 2006;47(11):4756-4761. Epub 2006/10/27. doi: 47/11/4756 [pii] 10.1167/iovs.06-0270. PubMed PMID: 17065484.
50. Lopes MC, Andrew T, Carbonaro F, Spector TD, Hammond CJ. Estimating heritability and shared environmental effects for refractive error in twin and family studies. Invest Ophthalmol Vis Sci. 2009;50(1):126-131. Epub 2008/09/02. doi: iovs.08-2385 [pii] 10.1167/iovs.08-2385. PubMed PMID: 18757506.

51. Verhoeven VJ, Hysi PG, Wojciechowski R, Fan Q, Guggenheim JA, Hohn R, et al. Genome-wide meta-analyses of multiancestry cohorts identify multiple new susceptibility loci for refractive error and myopia. Nat Genet. 2013;45(3):314-318. doi: 10.1038/ng.2554. PubMed PMID: 23396134.
52. Kiefer AK, Tung JY, Do CB, Hinds DA, Mountain JL, Francke U, et al. Genome-wide analysis points to roles for extracellular matrix remodeling, the visual cycle, and neuronal development in myopia. PLoS Genet. 2013;9(2):e1003299. doi: 10.1371/journal.pgen.1003299. PubMed PMID: 23468642; PubMed Central PMCID: PMC3585144.
53. Flitcroft DI, Loughman J, Wildsoet CF, Williams C, Guggenheim JA, for the CC. Novel Myopia Genes and Pathways Identified From Syndromic Forms of Myopia. Invest Ophthalmol Vis Sci. 2018;59(1):338-348. Epub 2018/01/19. doi: 10.1167/iovs.17-22173. PubMed PMID: 29346494; PubMed Central PMCID: PMCPMC5773233.
54. Tedja MS, Wojciechowski R, Hysi PG, Eriksson N, Furlotte NA, Verhoeven VJM, et al. Genome-wide association meta-analysis highlights light-induced signaling as a driver for refractive error. Nat Genet. 2018;50(6):834-848. Epub 2018/05/29. doi: 10.1038/s41588-018-0127-7. PubMed PMID: 29808027; PubMed Central PMCID: PMCPMC5980758.
55. McGlinn AM, Baldwin DA, Tobias JW, Budak MT, Khurana TS, Stone RA. Form-deprivation myopia in chick induces limited changes in retinal gene expression. Invest Ophthalmol Vis Sci. 2007;48(8):3430-3436. Epub 2007/07/27. doi: 48/8/3430 [pii] 10.1167/iovs.06-1538. PubMed PMID: 17652709; PubMed Central PMCID: PMC1983368.
56. Brand C, Schaeffel F, Feldkaemper MP. A microarray analysis of retinal transcripts that are controlled by image contrast in mice. Mol Vis. 2007;13:920-932. Epub 2007/07/27. doi: v13/a98 [pii]. PubMed PMID: 17653032.
57. Shelton L, Troilo D, Lerner MR, Gusev Y, Brackett DJ, Rada JS. Microarray analysis of choroid/RPE gene expression in marmoset eyes undergoing changes in ocular growth and refraction. Mol Vis. 2008;14:1465-1479. Epub 2008/08/14. PubMed PMID: 18698376; PubMed Central PMCID: PMC2504533.
58. Schippert R, Schaeffel F, Feldkaemper MP. Microarray analysis of retinal gene expression in chicks during imposed myopic defocus. Mol Vis. 2008;14:1589-1599. Epub 2008/09/05. PubMed PMID: 18769560; PubMed Central PMCID: PMC2528026.
59. Frost MR, Norton TT. Alterations in protein expression in tree shrew sclera during development of lens-induced myopia and recovery. Invest Ophthalmol Vis Sci. 2012;53(1):322-336. doi: 10.1167/iovs.11-8354. PubMed PMID: 22039233; PubMed Central PMCID: PMC3292368.
60. Gao H, Frost MR, Siegwart JT, Jr., Norton TT. Patterns of mRNA and protein expression during minus-lens compensation and recovery in tree shrew sclera. Mol Vis. 2011;17:903-919. PubMed PMID: 21541268; PubMed Central PMCID: PMC3084222.
61. Siegwart JT, Jr., Norton TT. The time course of changes in mRNA levels in tree shrew sclera during induced myopia and recovery. Invest Ophthalmol Vis Sci. 2002;43(7):2067-2075. Epub 2002/07/02. PubMed PMID: 12091398; PubMed Central PMCID: PMC1994662.
62. Riddell N, Giummarra L, Hall NE, Crewther SG. Bidirectional Expression of Metabolic, Structural, and Immune Pathways in Early Myopia and Hyperopia. Frontiers in neuroscience. 2016;10:390. doi: 10.3389/fnins.2016.00390. PubMed PMID: 27625591; PubMed Central PMCID: PMCPMC5003873.

63. Riddell N, Crewther SG. Integrated Comparison of GWAS, Transcriptome, and Proteomics Studies Highlights Similarities in the Biological Basis of Animal and Human Myopia. Invest Ophthalmol Vis Sci. 2017;58(1):660-669. Epub 2017/01/31. doi: 10.1167/iovs.16-20618. PubMed PMID: 28135361.
64. Churchill GA, Airey DC, Allayee H, Angel JM, Attie AD, Beatty J, et al. The Collaborative Cross, a community resource for the genetic analysis of complex traits. Nat Genet. 2004;36(11):1133-1137. doi: 10.1038/ng1104-1133. PubMed PMID: 15514660.
65. Tkatchenko TV, Shen Y, Tkatchenko AV. Analysis of postnatal eye development in the mouse with high-resolution small animal magnetic resonance imaging. Invest Ophthalmol Vis Sci. 2010;51(1):21-27. Epub 2009/08/08. doi: iovs.08-2767 [pii] 10.1167/iovs.08-2767. PubMed PMID: 19661239.
66. Shah RL, Guggenheim JA, Eye UKB, Vision C. Genome-wide association studies for corneal and refractive astigmatism in UK Biobank demonstrate a shared role for myopia susceptibility loci. Hum Genet. 2018;137(11-12):881-896. Epub 2018/10/12. doi: 10.1007/s00439-018-1942-8. PubMed PMID: 30306274; PubMed Central PMCID: PMCPMC6267700.
67. Tkatchenko TV, Troilo D, Benavente-Perez A, Tkatchenko AV. Gene expression in response to optical defocus of opposite signs reveals bidirectional mechanism of visually guided eye growth. PLoS Biol. 2018;16(10):e2006021. Epub 2018/10/10. doi: 10.1371/journal.pbio.2006021. PubMed PMID: 30300342; PubMed Central PMCID: PMCPMC6177118.
68. Riddell N, Crewther SG. Novel evidence for complement system activation in chick myopia and hyperopia models: a meta-analysis of transcriptome datasets. Scientific reports. 2017;7(1):9719. doi: 10.1038/s41598-017-10277-2. PubMed PMID: 28852117; PubMed Central PMCID: PMCPMC5574905.
69. Stone RA, McGlinn AM, Baldwin DA, Tobias JW, Iuvone PM, Khurana TS. Image defocus and altered retinal gene expression in chick: clues to the pathogenesis of ametropia. Invest Ophthalmol Vis Sci. 2011;52(8):5765-5777. doi: 10.1167/iovs.10-6727. PubMed PMID: 21642623; PubMed Central PMCID: PMCPMC3176046.
70. Ronquillo CC, Bernstein PS, Baehr W. Senior-Loken syndrome: a syndromic form of retinal dystrophy associated with nephronophthisis. Vision Res. 2012;75:88-97. Epub 2012/07/24. doi: 10.1016/j.visres.2012.07.003. PubMed PMID: 22819833; PubMed Central PMCID: PMCPMC3504181.
71. Marmorstein LY, Munier FL, Arsenijevic Y, Schorderet DF, McLaughlin PJ, Chung D, et al. Aberrant accumulation of EFEMP1 underlies drusen formation in Malattia Leventinese and age-related macular degeneration. Proc Natl Acad Sci U S A. 2002;99(20):13067-13072. Epub 2002/09/21. doi: 10.1073/pnas.202491599. PubMed PMID: 12242346; PubMed Central PMCID: PMCPMC130587.
72. Tuschl K, Clayton PT, Gospe SM, Jr., Gulab S, Ibrahim S, Singhi P, et al. Syndrome of hepatic cirrhosis, dystonia, polycythemia, and hypermanganesemia caused by mutations in SLC30A10, a manganese transporter in man. Am J Hum Genet. 2012;90(3):457-466. Epub 2012/02/22. doi: 10.1016/j.ajhg.2012.01.018. PubMed PMID: 22341972; PubMed Central PMCID: PMCPMC3309187.
73. Leyva-Illades D, Chen P, Zogzas CE, Hutchens S, Mercado JM, Swaim CD, et al. SLC30A10 is a cell surface-localized manganese efflux transporter, and parkinsonism-causing mutations block its intracellular trafficking and efflux activity. J Neurosci. 2014;34(42):14079-14095.

Epub 2014/10/17. doi: 10.1523/JNEUROSCI.2329-14.2014. PubMed PMID: 25319704; PubMed Central PMCID: PMCPMC4198546.

74. Papal S, Monti CE, Tennison ME, Swaroop A. Molecular dissection of cone photoreceptor-enriched genes encoding transmembrane and secretory proteins. J Neurosci Res. 2019;97(1):16-28. Epub 2018/09/28. doi: 10.1002/jnr.24329. PubMed PMID: 30260491; PubMed Central PMCID: PMCPMC6239890.
75. Paridaen JT, Janson E, Utami KH, Pereboom TC, Essers PB, van Rooijen C, et al. The nucleolar GTP-binding proteins Gnl2 and nucleostemin are required for retinal neurogenesis in developing zebrafish. Dev Biol. 2011;355(2):286-301. Epub 2011/05/14. doi: 10.1016/j.ydbio.2011.04.028. PubMed PMID: 21565180.
76. MacDonald R, Barbat-Artigas S, Cho C, Peng H, Shang J, Moustaine A, et al. A Novel Egr-1-Agrin Pathway and Potential Implications for Regulation of Synaptic Physiology and Homeostasis at the Neuromuscular Junction. Front Aging Neurosci. 2017;9:258. Epub 2017/08/22. doi: 10.3389/fnagi.2017.00258. PubMed PMID: 28824419; PubMed Central PMCID: PMCPMC5541023.
77. Mann S, Kroger S. Agrin is synthesized by retinal cells and colocalizes with gephyrin [corrected]. Mol Cell Neurosci. 1996;8(1):1-13. Epub 1996/01/01. PubMed PMID: 8923451.
78. Tkatchenko TV, Tkatchenko AV. Ketamine-xylazine anesthesia causes hyperopic refractive shift in mice. J Neurosci Methods. 2010;193(1):67-71. Epub 2010/09/04. doi: S0165-0270(10)00411-5 [pii] 10.1016/j.jneumeth.2010.07.036. PubMed PMID: 20813132; PubMed Central PMCID: PMC2952685.
79. Tkatchenko TV, Shen Y, Tkatchenko AV. Mouse experimental myopia has features of primate myopia. Invest Ophthalmol Vis Sci. 2010;51(3):1297-1303. Epub 2009/10/31. doi: iovs.09-4153 [pii] 10.1167/iovs.09-4153. PubMed PMID: 19875658.
80. Tkatchenko TV, Shen Y, Braun RD, Bawa G, Kumar P, Avrutsky I, et al. Photopic visual input is necessary for emmetropization in mice. Exp Eye Res. 2013;115C:87-95. doi: 10.1016/j.exer.2013.06.025. PubMed PMID: 23838522.
81. Storey JD, Tibshirani R. Statistical significance for genomewide studies. Proc Natl Acad Sci U S A. 2003;100(16):9440-9445. Epub 2003/07/29. doi: 10.1073/pnas.1530509100. PubMed PMID: 12883005; PubMed Central PMCID: PMCPMC170937.
82. Huang da W, Sherman BT, Lempicki RA. Systematic and integrative analysis of large gene lists using DAVID bioinformatics resources. Nat Protoc. 2009;4(1):44-57. Epub 2009/01/10. doi: nprot.2008.211 [pii] 10.1038/nprot.2008.211. PubMed PMID: 19131956.
83. Walter W, Sanchez-Cabo F, Ricote M. GOplot: an R package for visually combining expression data with functional analysis. Bioinformatics. 2015;31(17):2912-2914. Epub 2015/05/13. doi: 10.1093/bioinformatics/btv300. PubMed PMID: 25964631.
84. de Leeuw CA, Mooij JM, Heskes T, Posthuma D. MAGMA: generalized gene-set analysis of GWAS data. PLoS Comput Biol. 2015;11(4):e1004219. Epub 2015/04/18. doi: 10.1371/journal.pcbi.1004219. PubMed PMID: 25885710; PubMed Central PMCID: PMCPMC4401657.

Figure legends

Fig 1. Genetic background modulates refractive eye development and susceptibility to myopia in mice. (**A**) Refractive error is inherited as a quantitative trait in the founder strains of Collaborative Cross. Baseline refractive errors at P40 range from highly myopic to highly hyperopic depending on the genetic background in different strains. Horizontal red lines show mean refractive errors for each strain, while each dot corresponds to mean refractive errors of individual animals. (**B**) Susceptibility to form-deprivation myopia is inherited as a quantitative trait in the founder strains of Collaborative Cross. The extent of myopia induced by 21 days of visual form deprivation in different strains ranged from -5.5 ± 2.1 D in NZO/HlLtJ mice to -18.7 ± 3.1 D in CAST/EiJ mice. Horizontal red lines identify means of induced myopia for each strain, while each dot represents a mean interocular difference between deprived eye and control contralateral eye for individual animals.

Fig 2. Baseline refractive eye development in mice is regulated by a large number of genes via multiple retinal signaling pathways. (**A**) Expression of 2,302 retinal genes correlates with baseline refractive error in mice. Hierarchical clustering results show that genes, whose expression correlates with refractive error in the founder strains of Collaborative Cross, are organized in two clusters, i.e., one (top) cluster exhibiting increased expression in the highly hyperopic mice, and the second (bottom) cluster showing increased expression in the myopic mice. (**B**) Top fifteen

biological processes affected by the genes whose expression correlates with the baseline refractive errors in the founder strains of Collaborative Cross. Outer circle shows gene ontology IDs for the biological processes; second circle shows up- or down-regulated genes in the myopic mice versus hyperopic mice; inner circle shows activation or suppression of the corresponding biological processes, while the size of the sector corresponds to statistical significance (larger sectors correspond to smaller *P*-values). (**C**) Top twenty-five canonical pathways affected by the genes whose expression correlates with the baseline refractive errors in the founder strains of Collaborative Cross. Horizontal yellow line indicates $P = 0.05$. Z-score shows activation or suppression of the corresponding pathways.

Fig 3. Susceptibility to myopia in mice is regulated by a large number of genes via multiple retinal signaling pathways. (**A**) Expression of 1,917 retinal genes correlates with susceptibility to form deprivation myopia in mice. Hierarchical clustering results show that genes, whose expression correlates with susceptibility to myopia in the founder strains of Collaborative Cross, are organized in two clusters, i.e., one (top) cluster exhibiting increased expression in mice with high susceptibility to myopia, and the second (bottom) cluster showing increased expression in mice with low susceptibility to myopia. (**B**) Top fifteen biological processes affected by the genes whose expression correlates with susceptibility to myopia in the founder strains of Collaborative Cross. Outer circle shows gene ontology IDs for the biological processes; second circle shows up- or down-regulated genes in mice with high susceptibility to myopia versus mice with low susceptibility to myopia; inner circle shows activation or suppression of the corresponding biological processes, while the size of the sector corresponds to statistical significance (larger sectors correspond to smaller *P*-values). (**C**) Top twenty-five canonical pathways affected by the

genes whose expression correlates with susceptibility to myopia in the founder strains of Collaborative Cross. Horizontal yellow line indicates $P = 0.05$. Z-score shows activation or suppression of the corresponding pathways.

Fig 4. Baseline refractive eye development and susceptibility to myopia in mice are regulated via overlapping pathways. (**A**) Venn diagram showing substantial overlap between genes underlying baseline refractive eye development and genes regulating susceptibility to myopia in Collaborative Cross progenitor strain mice. (**B**) Top fifteen biological processes affected by the 714 genes associated with both baseline refractive eye development (top panel) and susceptibility to myopia in mice (bottom panel). Outer circle shows gene ontology IDs for the biological processes; second circle shows up- or down-regulated genes in the myopic mice versus hyperopic mice (top panel), or in mice with high susceptibility to form-deprivation myopia versus mice with low susceptibility to myopia (bottom panel); inner circle shows activation or suppression of the corresponding biological processes, while the size of the sector corresponds to statistical significance (larger sectors correspond to smaller *P*-values). (**C**) Top twenty-five canonical pathways affected by the 714 genes involved in the regulation of both baseline refractive eye development (top panel) and susceptibility to myopia (bottom panel) in the founder strains of Collaborative Cross. Horizontal yellow line indicates $P = 0.05$. Z-score shows activation or suppression of the corresponding pathways.

Fig 5. Summary of signaling pathways involved in regulation of baseline refractive eye development and susceptibility to myopia. Heatmap showing all statistically significant canonical pathways ($P < 0.05$) affected by the 2,302 genes involved in baseline refractive

development (left panel), 1,917 genes influencing susceptibility to myopia (right panel), and 714 genes underlying both baseline refractive development and susceptibility to myopia (two panels in the middle). Z-score shows activation or suppression of the corresponding pathways.

Fig 6. Genes localized within human myopia QTLs show functional overlap with genes underlying baseline refractive eye development and susceptibility to myopia in mice. 750 candidate genes localized within 279 human myopia QTLs exhibit statistically significant overlap with both genes involved in baseline refractive eye development and genes regulating susceptibility to myopia in Collaborative Cross progenitor strain mice.

Fig 7. Genes underlying baseline refractive eye development and susceptibility to myopia in mice are localized in human QTLs associated with myopia (part 1). Heatmap depicting genes and odds ratios for the overlaps between 109 human myopia QTLs and genes whose expression correlates with either baseline refractive errors, susceptibility to form deprivation myopia, or both in mice. Colors indicate odds ratios. Bold italic identifies genes found to be associated with refractive error in UK Biobank, CREAM, or both human samples by the gene-based genome-wide association analysis. Red identifies genes exhibiting correlation with both baseline refractive development and susceptibility to myopia in mice.

Fig 8. Genes underlying baseline refractive eye development and susceptibility to myopia in mice are localized in human QTLs associated with myopia (part 2). Heatmap depicting genes and odds ratios for the overlaps between 109 human myopia QTLs and genes whose expression correlates with either baseline refractive errors, susceptibility to form deprivation myopia, or both

in mice. Colors indicate odds ratios. Bold italic identifies genes found to be associated with refractive error in UK Biobank, CREAM, or both human samples by the gene-based genome-wide association analysis. Red identifies genes exhibiting correlation with both baseline refractive development and susceptibility to myopia in mice.

Fig 9. Top biological processes associated with genes linked to refractive eye development in mice and localized in known human myopia QTLs. (**A**) Chord diagram showing key genes (left semicircle) and top biological processes (right semicircle) associated with genes correlated with baseline refractive development in mice and localized in known human QTLs linked to myopia. (**B**) Chord diagram showing key genes (left semicircle) and top biological processes (right semicircle) for genes correlated with susceptibility to myopia in mice and localized in known human QTLs linked to myopia. Colored bars underneath gene names show up- or down-regulation of corresponding genes in either myopic mice versus hyperopic mice (A), or mice with high susceptibility to myopia versus mice with low susceptibility to myopia (B).

Fig 10. Summary of key biological processes and pathways affected by genes underlying refractive eye development and found to be linked to myopia in UK Biobank and CREAM human cohorts. (**A**) Hierarchical clustering diagram showing top 30 biological processes affected by genes underlying baseline refractive eye development in humans. Outer circle shows hierarchical clusters of biological processes (identified by different colors) linked to baseline refractive development; inner circle shows clusters of the corresponding genes up- or down-regulated in myopic mice versus hyperopic mice. (**B**) Top twenty-five canonical pathways affected

by the genes underlying baseline refractive eye development in humans. Horizontal yellow line indicates $P = 0.05$. Z-score shows activation or suppression of the corresponding pathways.

Fig 11. Summary of key biological processes and pathways affected by genes regulating susceptibility to myopia and found to be linked to myopia in UK Biobank and CREAM human cohorts. (**A**) Hierarchical clustering diagram showing top 30 biological processes affected by genes regulating susceptibility to myopia in humans. Outer circle shows hierarchical clusters of biological processes (identified by different colors) underlying regulation of susceptibility to myopia; inner circle shows clusters of the corresponding genes up- or down-regulated in mice with high susceptibility to myopia versus mice with low susceptibility to myopia. (**B**) Top twenty-five canonical pathways affected by the genes regulating susceptibility to myopia in humans. Horizontal yellow line indicates $P = 0.05$. Z-score shows activation or suppression of the corresponding pathways.

Supporting information

S1 Table. Baseline refractive errors in Collaborative Cross mice measured at P40 (diopters).

S2 Table. Form-deprivation myopia in Collaborative Cross mice (deprived eye versus control eye, diopters).

S3 Table. List of genes whose expression correlates with baseline refractive error in Collaborative Cross mice.

S4 Table. Gene ontology categories significantly associated with genes whose expression correlates with baseline refractive error in Collaborative Cross mice (BP, biological process; CC, cellular component; MF, molecular function).

S5 Table. Canonical signaling pathways affected by genes whose expression correlates with baseline refractive error in Collaborative Cross mice.

S6 Table. List of genes whose expression correlates with susceptibility to myopia in Collaborative Cross mice.

S7 Table. Gene ontology categories significantly associated with genes whose expression correlates with susceptibility to myopia in Collaborative Cross mice (BP, biological process; CC, cellular component; MF, molecular function).

S8 Table. Canonical signaling pathways affected by genes whose expression correlates with susceptibility to myopia in Collaborative Cross mice.

S9 Table. List of genes whose expression correlates with both baseline refractive error and susceptibility to myopia in Collaborative Cross mice.

S10 Table. Gene ontology categories significantly associated with genes whose expression correlates with both baseline refractive error and susceptibility to myopia in Collaborative Cross mice (BP, biological process; CC, cellular component; MF, molecular function).

S11 Table. Canonical signaling pathways affected by genes whose expression correlates with both baseline refractive error and susceptibility to myopia in Collaborative Cross mice.

S12 Table. List of human myopia QTLs and candidate genes located within 200 kb of the lead SNP (or within critical region).

S13 Table. List of genes localized within human myopia QTLs and whose expression correlates with baseline refractive error in mice.

S14 Table. List of genes localized within human myopia QTLs and whose expression correlates with susceptibility to myopia in mice.

S15 Table. List of genes localized within human myopia QTLs and whose expression correlates with both baseline refractive error and susceptibility to myopia in mice.

S16 Table. List of human myopia QTLs showing overlap with genes exhibiting correlation with either refractive error or susceptibility to myopia in mice.

S17 Table. Gene ontology categories significantly associated with genes localized within human myopia QTLs and whose expression correlates with baseline refractive error in mice (BP, biological process; CC, cellular component; MF, molecular function).

S18 Table. Gene ontology categories significantly associated with genes localized within human myopia QTLs and whose expression correlates with susceptibility to myopia in mice (BP, biological process; CC, cellular component; MF, molecular function).

S19 Table. List of mouse genes displaying significant association with refractive error in CREAM cohort and whose expression correlates with baseline refractive error in mice (Blue identifies $P_{Bonferroni} < 0.05$ in both cohorts).

S20 Table. List of mouse genes displaying significant association with refractive error in UK Biobank cohort and whose expression correlates with baseline refractive error in mice (Blue identifies $P_{Bonferroni} < 0.05$ in both cohorts).

S21 Table. List of mouse genes displaying significant association with refractive error in CREAM cohort and whose expression correlates with susceptibility to myopia in mice (Blue identifies $P_{Bonferroni} < 0.05$ in both cohorts).

S22 Table. List of mouse genes displaying significant association with refractive error in UK Biobank cohort and whose expression correlates with susceptibility to myopia in mice (Blue identifies $P_{Bonferroni} < 0.05$ in both cohorts).

S23 Table. List of mouse genes displaying significant association with refractive error in both UK Biobank and CREAM cohorts, and whose expression correlates with baseline refractive error in mice (Blue identifies $P_{Bonferroni} < 0.05$ in both cohorts).

S24 Table. List of mouse genes displaying significant association with refractive error in both UK Biobank and CREAM cohorts, and whose expression correlates with susceptibility to myopia in mice (Blue identifies $P_{Bonferroni} < 0.05$ in both cohorts).

S25 Table. Biological processes significantly associated with genes linked to refractive error in UK Biobank and CREAM cohorts, and whose expression correlates with baseline refractive error in mice (BP, biological process).

S26 Table. Biological processes significantly associated with genes linked to refractive error in UK Biobank and CREAM cohorts, and whose expression correlates with susceptibility to myopia in mice (BP, biological process).

S27 Table. Canonical signaling pathways significantly associated with genes linked to refractive error in UK Biobank and CREAM cohorts, and whose expression correlates with baseline refractive error in mice.

S28 Table. Canonical signaling pathways significantly associated with genes linked to refractive error in UK Biobank and CREAM cohorts, and whose expression correlates with susceptibility to myopia in mice.

S1 Text. List of CREAM consortium members and their affiliations.

S2 Text. List of UK Biobank Eye and Vision Consortium members and their affiliations.

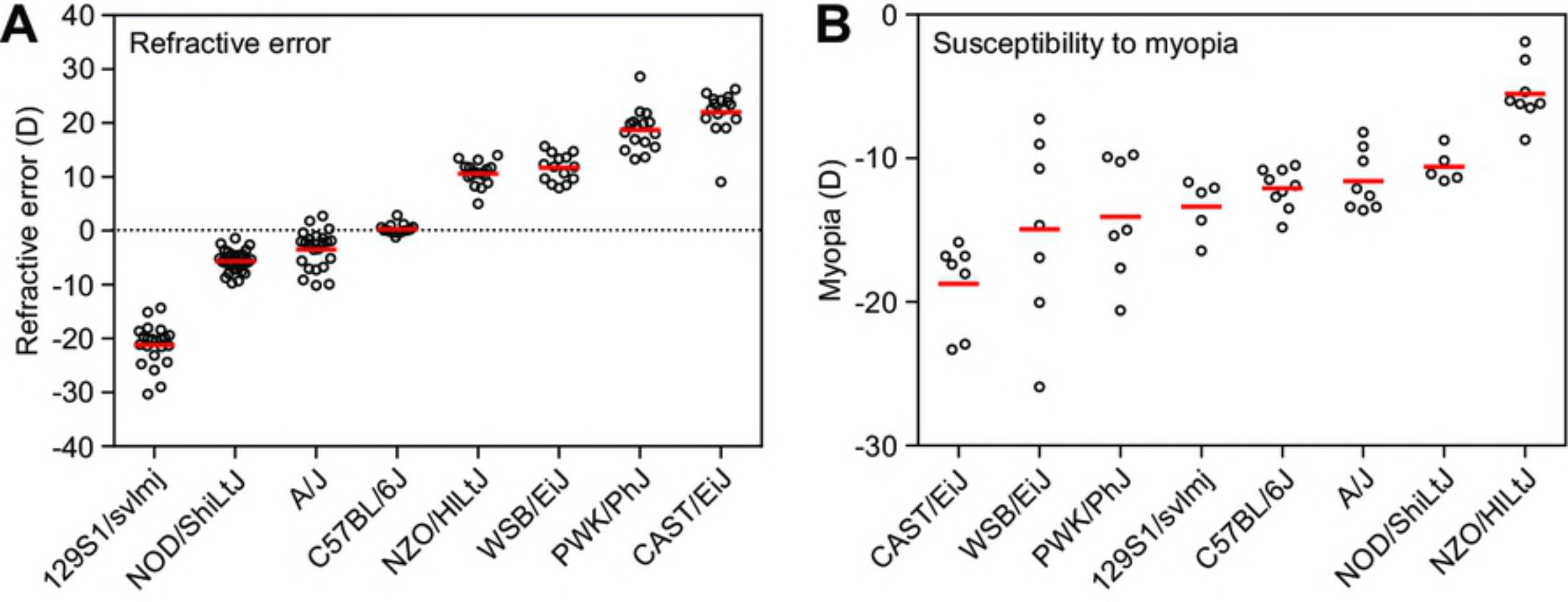
A
Refractive error
Refractive error (D)
40
30
20
10
0
-10
-20
-30
-40
129S1/svlmj
NOD/ShiLtJ
A/J
C57BL/6J
NZO/HILtJ
WSB/EiJ
PWK/PhJ
CAST/EiJ
B
Susceptibility to myopia
Myopia (D)
0
-10
-20
-30
CAST/EiJ
WSB/EiJ
PWK/PhJ
129S1/svlmj
C57BL/6J
A/J
NOD/ShiLtJ
NZO/HILtJ

Figure 1

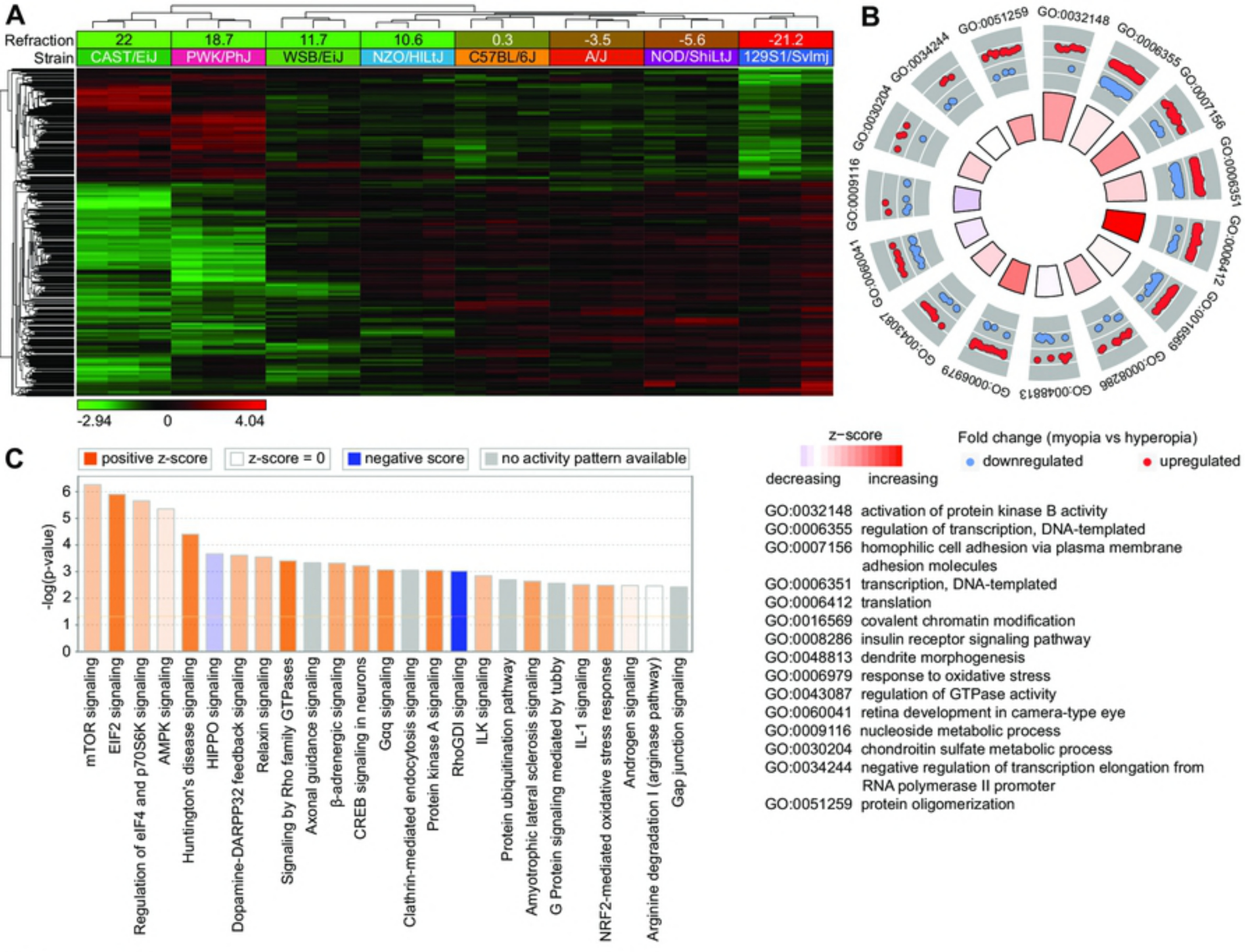

GO:0032148	activation of protein kinase B activity
GO:0006355	regulation of transcription, DNA-templated
GO:0007156	homophilic cell adhesion via plasma membrane adhesion molecules
GO:0006351	transcription, DNA-templated
GO:0006412	translation
GO:0016569	covalent chromatin modification
GO:0008286	insulin receptor signaling pathway
GO:0048813	dendrite morphogenesis
GO:0006979	response to oxidative stress
GO:0043087	regulation of GTPase activity
GO:0060041	retina development in camera-type eye
GO:0009116	nucleoside metabolic process
GO:0030204	chondroitin sulfate metabolic process
GO:0034244	negative regulation of transcription elongation from RNA polymerase II promoter
GO:0051259	protein oligomerization

Figure 2

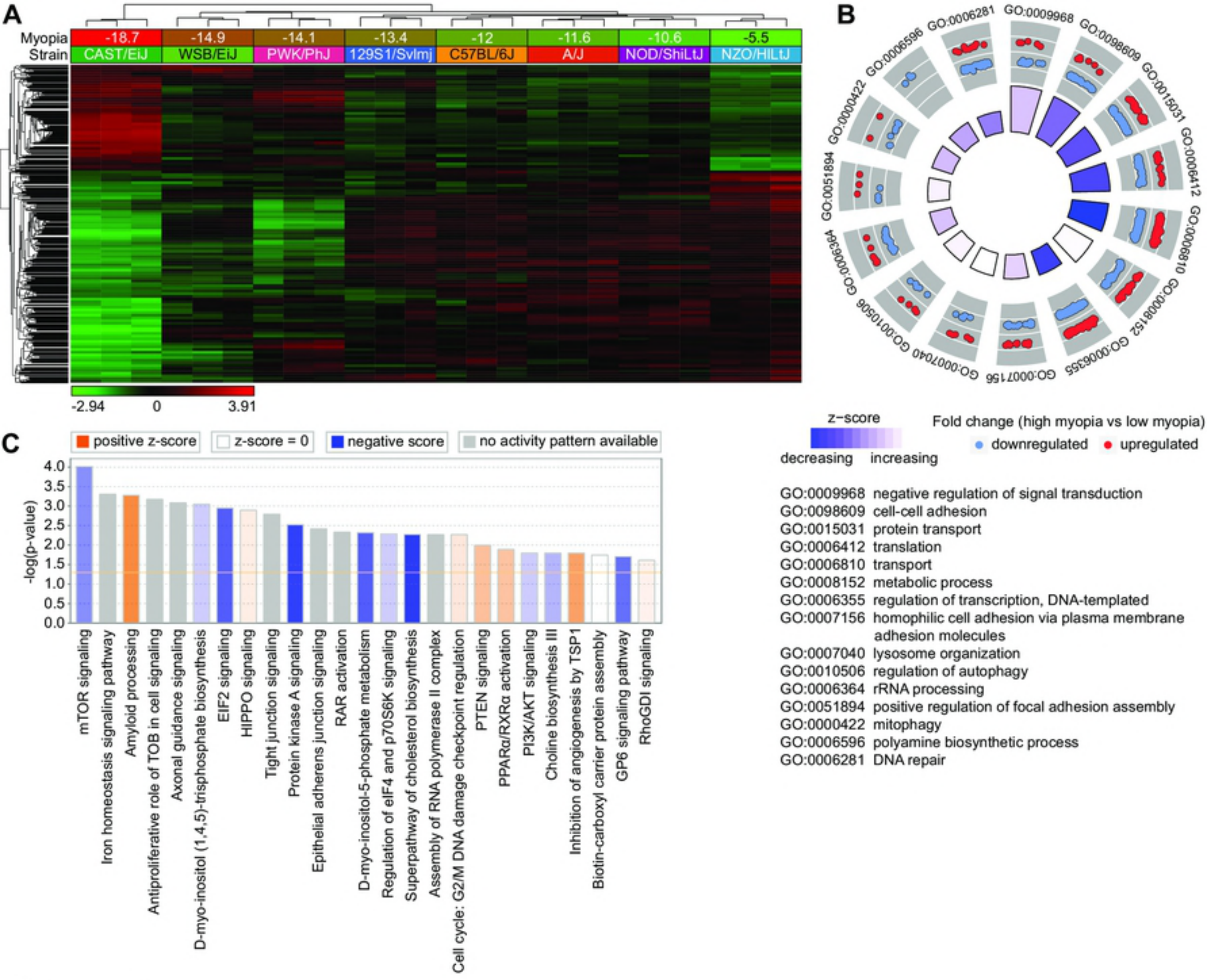
A
Myopia
Strain
-18.7
CAST/EiJ
-14.9
WSB/EiJ
-14.1
PWK/PhJ
-13.4
129S1/SvImj
-12
C57BL/6J
-11.6
A/J
-10.6
NOD/ShiLtJ
-5.5
NZO/HILtJ
-2.94
0
3.91
B
GO:0009968
GO:0098609
GO:0015031
GO:0006412
GO:0006810
GO:0008152
GO:0006355
GO:0007156
GO:0007040
GO:0010506
GO:0006364
GO:0051894
GO:0000422
GO:0006596
GO:0006281
z-score
decreasing
increasing
Fold change (high myopia vs low myopia)
downregulated
upregulated
C
positive z-score
z-score = 0
negative score
no activity pattern available
-log(p-value)
4.0
3.5
3.0
2.5
2.0
1.5
1.0
0.5
0.0
mTOR signaling
Iron homeostasis signaling pathway
Amyloid processing
Antiproliferative role of TOB in cell signaling
Axonal guidance signaling
D-myo-inositol (1,4,5)-trisphosphate biosynthesis
EIF2 signaling
HIPPO signaling
Tight junction signaling
Protein kinase A signaling
Epithelial adherens junction signaling
RAR activation
D-myo-inositol-5-phosphate metabolism
Regulation of eIF4 and p70S6K signaling
Superpathway of cholesterol biosynthesis
Assembly of RNA polymerase II complex
Cell cycle: G2/M DNA damage checkpoint regulation
PTEN signaling
PPARα/RXRα activation
PI3K/AKT signaling
Choline biosynthesis III
Inhibition of angiogenesis by TSP1
Biotin-carboxyl carrier protein assembly
GP6 signaling pathway
RhoGDI signaling
GO:0009968 negative regulation of signal transduction
GO:0098609 cell-cell adhesion
GO:0015031 protein transport
GO:0006412 translation
GO:0006810 transport
GO:0008152 metabolic process
GO:0006355 regulation of transcription, DNA-templated
GO:0007156 homophilic cell adhesion via plasma membrane adhesion molecules
GO:0007040 lysosome organization
GO:0010506 regulation of autophagy
GO:0006364 rRNA processing
GO:0051894 positive regulation of focal adhesion assembly
GO:0000422 mitophagy
GO:0006596 polyamine biosynthetic process
GO:0006281 DNA repair

Figure 3

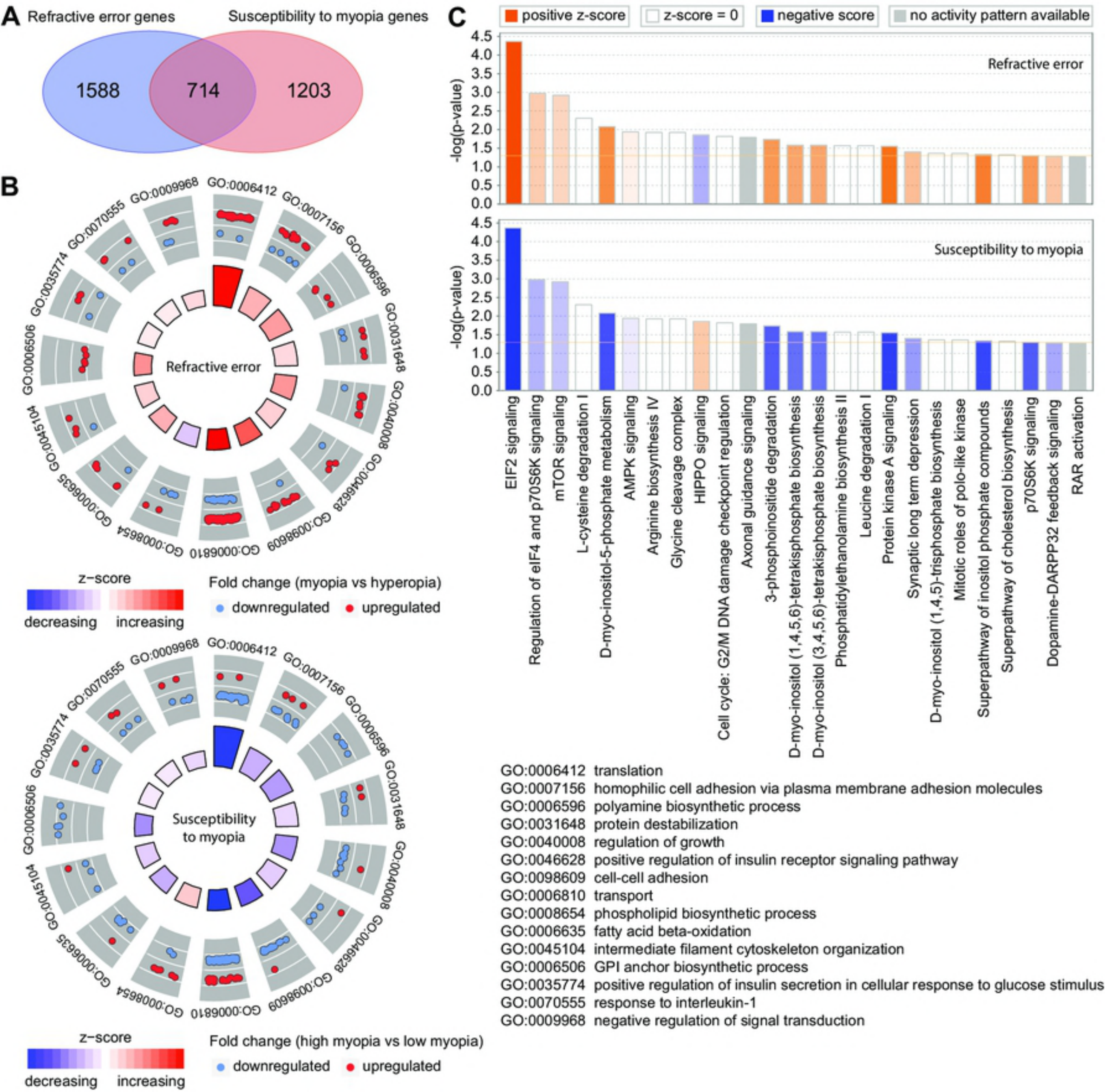

GO:0006412 translation
GO:0007156 homophilic cell adhesion via plasma membrane adhesion molecules
GO:0006596 polyamine biosynthetic process
GO:0031648 protein destabilization
GO:0040008 regulation of growth
GO:0046628 positive regulation of insulin receptor signaling pathway
GO:0098609 cell-cell adhesion
GO:0006810 transport
GO:0008654 phospholipid biosynthetic process
GO:0006635 fatty acid beta-oxidation
GO:0045104 intermediate filament cytoskeleton organization
GO:0006506 GPI anchor biosynthetic process
GO:0035774 positive regulation of insulin secretion in cellular response to glucose stimulus
GO:0070555 response to interleukin-1
GO:0009968 negative regulation of signal transduction

Figure 4

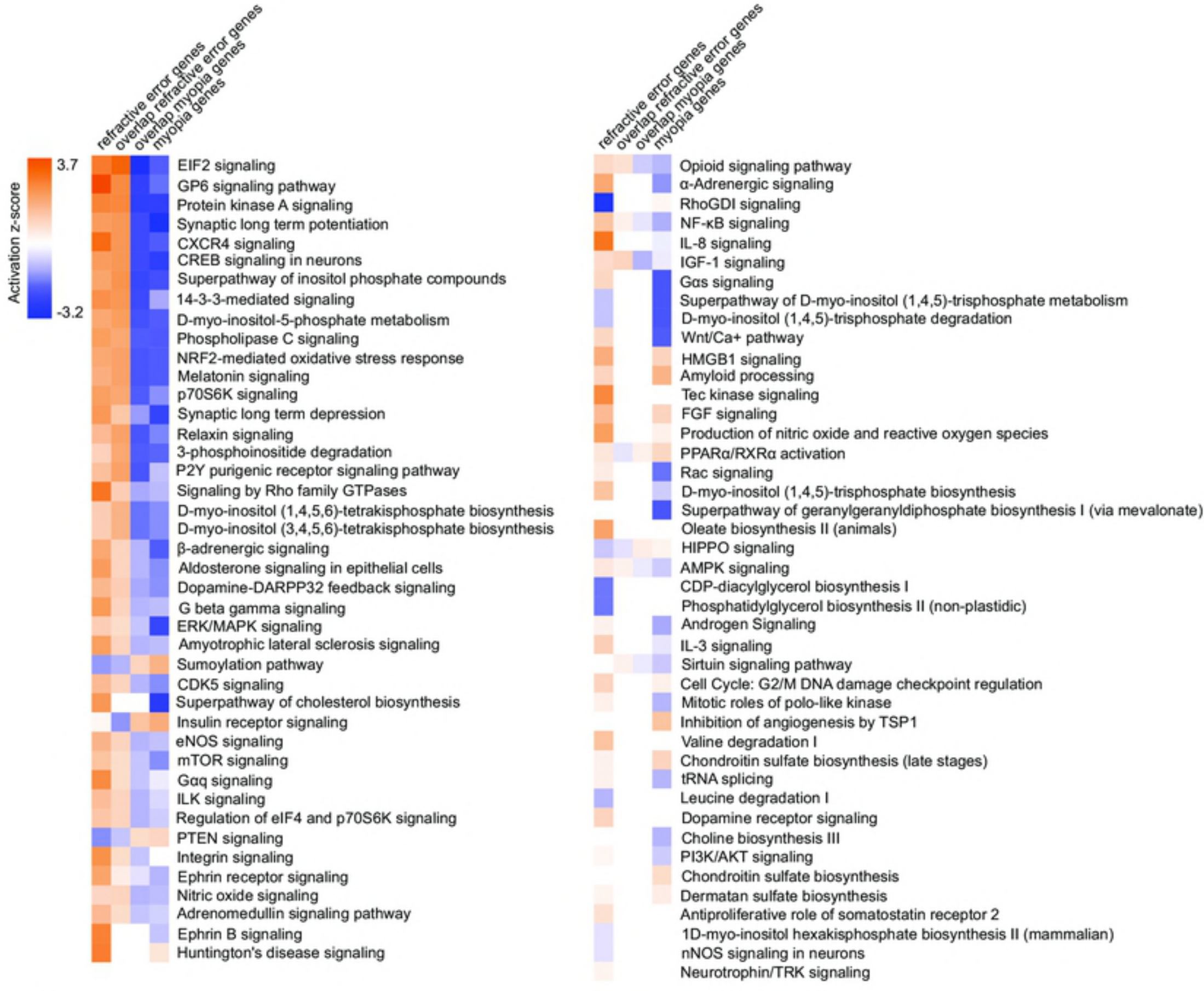
refractive error genes
overlap refractive error genes
overlap myopia genes
myopia genes
Activation z-score
3.7
-3.2
EIF2 signaling
GP6 signaling pathway
Protein kinase A signaling
Synaptic long term potentiation
CXCR4 signaling
CREB signaling in neurons
Superpathway of inositol phosphate compounds
14-3-3-mediated signaling
D-myo-inositol-5-phosphate metabolism
Phospholipase C signaling
NRF2-mediated oxidative stress response
Melatonin signaling
p70S6K signaling
Synaptic long term depression
Relaxin signaling
3-phosphoinositide degradation
P2Y purigenic receptor signaling pathway
Signaling by Rho family GTPases
D-myo-inositol (1,4,5,6)-tetrakisphosphate biosynthesis
D-myo-inositol (3,4,5,6)-tetrakisphosphate biosynthesis
β-adrenergic signaling
Aldosterone signaling in epithelial cells
Dopamine-DARPP32 feedback signaling
G beta gamma signaling
ERK/MAPK signaling
Amyotrophic lateral sclerosis signaling
Sumoylation pathway
CDK5 signaling
Superpathway of cholesterol biosynthesis
Insulin receptor signaling
eNOS signaling
mTOR signaling
Gαq signaling
ILK signaling
Regulation of eIF4 and p70S6K signaling
PTEN signaling
Integrin signaling
Ephrin receptor signaling
Nitric oxide signaling
Adrenomedullin signaling pathway
Ephrin B signaling
Huntington's disease signaling
refractive error genes
overlap refractive error genes
overlap myopia genes
myopia genes
Opioid signaling pathway
α-Adrenergic signaling
RhoGDI signaling
NF-κB signaling
IL-8 signaling
IGF-1 signaling
Gαs signaling
Superpathway of D-myo-inositol (1,4,5)-trisphosphate metabolism
D-myo-inositol (1,4,5)-trisphosphate degradation
Wnt/Ca+ pathway
HMGB1 signaling
Amyloid processing
Tec kinase signaling
FGF signaling
Production of nitric oxide and reactive oxygen species
PPARα/RXRα activation
Rac signaling
D-myo-inositol (1,4,5)-trisphosphate biosynthesis
Superpathway of geranylgeranyldiphosphate biosynthesis I (via mevalonate)
Oleate biosynthesis II (animals)
HIPPO signaling
AMPK signaling
CDP-diacylglycerol biosynthesis I
Phosphatidylglycerol biosynthesis II (non-plastidic)
Androgen Signaling
IL-3 signaling
Sirtuin signaling pathway
Cell Cycle: G2/M DNA damage checkpoint regulation
Mitotic roles of polo-like kinase
Inhibition of angiogenesis by TSP1
Valine degradation I
Chondroitin sulfate biosynthesis (late stages)
tRNA splicing
Leucine degradation I
Dopamine receptor signaling
Choline biosynthesis III
PI3K/AKT signaling
Chondroitin sulfate biosynthesis
Dermatan sulfate biosynthesis
Antiproliferative role of somatostatin receptor 2
1D-myo-inositol hexakisphosphate biosynthesis II (mammalian)
nNOS signaling in neurons
Neurotrophin/TRK signaling

Figure 5

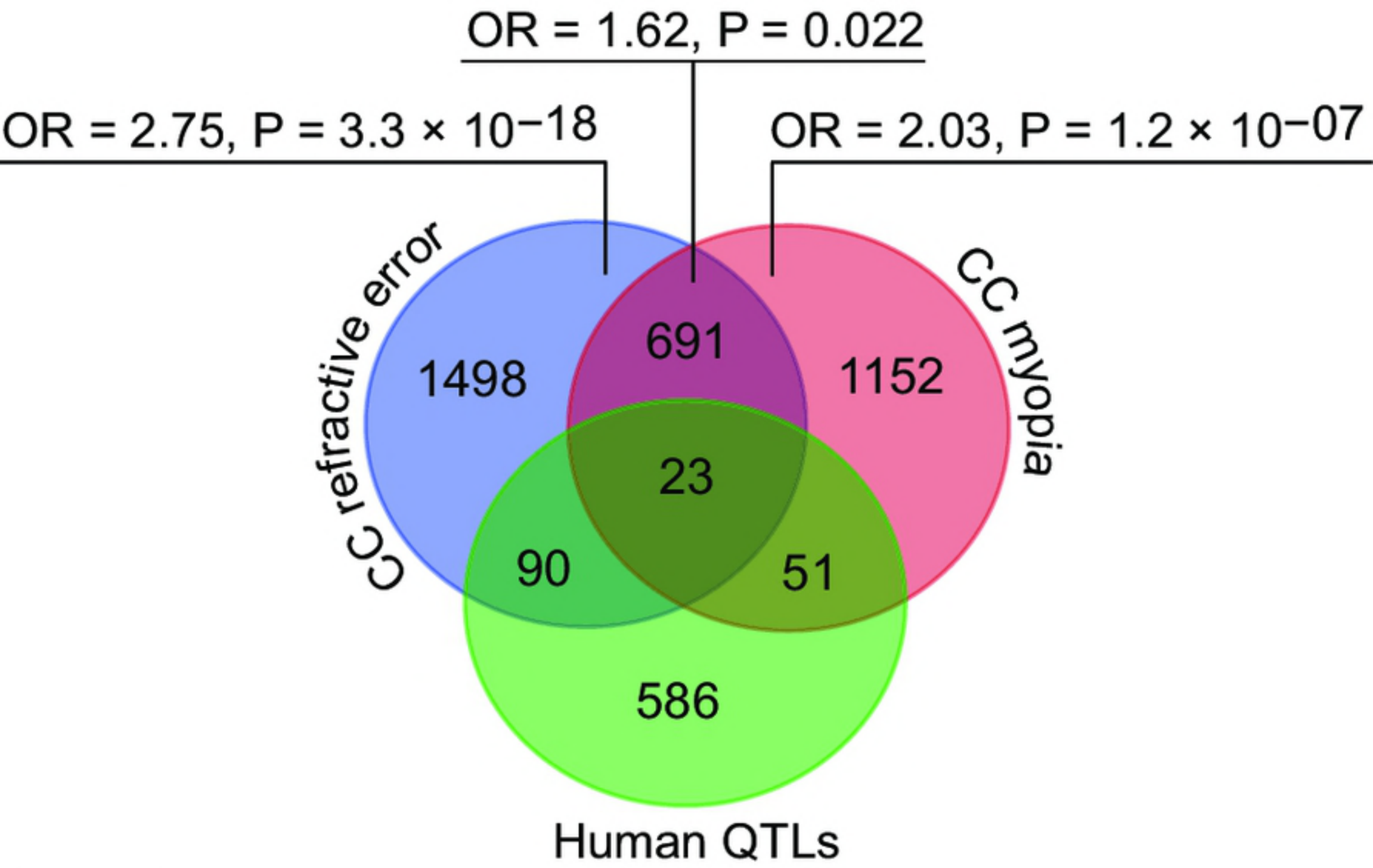
OR = 1.62, P = 0.022
OR = 2.75, P = 3.3 × 10−18
OR = 2.03, P = 1.2 × 10−07
CC refractive error
CC myopia
Human QTLs
1498
691
1152
23
90
51
586

Figure 6

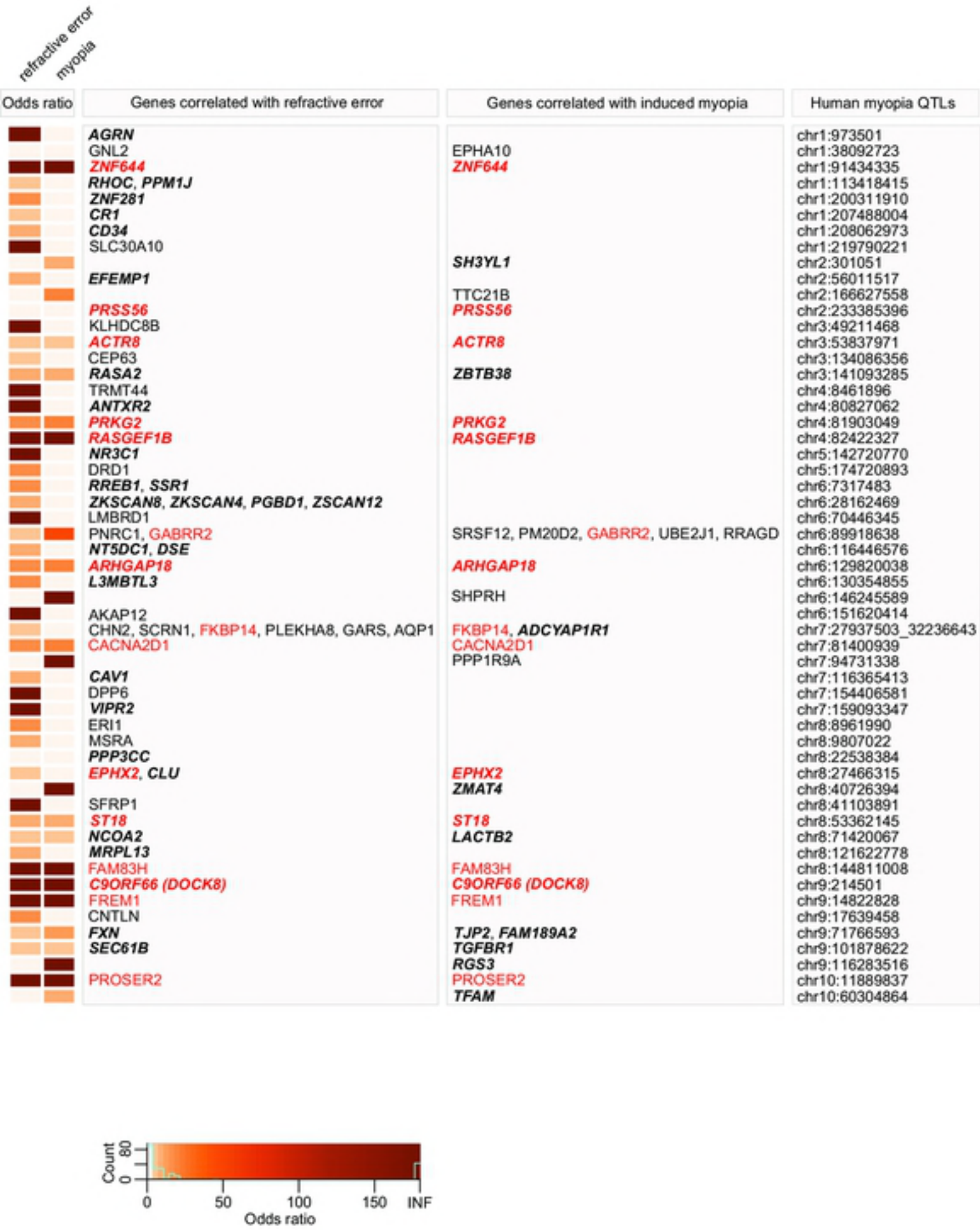
refractive error
myopia
Odds ratio
Genes correlated with refractive error
Genes correlated with induced myopia
Human myopia QTLs
AGRN
GNL2
ZNF644
RHOC, PPM1J
ZNF281
CR1
CD34
SLC30A10
EFEMP1
PRSS56
KLHDC8B
ACTR8
CEP63
RASA2
TRMT44
ANTXR2
PRKG2
RASGEF1B
NR3C1
DRD1
RREB1, SSR1
ZKSCAN8, ZKSCAN4, PGBD1, ZSCAN12
LMBRD1
PNRC1, GABRR2
NT5DC1, DSE
ARHGAP18
L3MBTL3
AKAP12
CHN2, SCRN1, FKBP14, PLEKHA8, GARS, AQP1
CACNA2D1
CAV1
DPP6
VIPR2
ERI1
MSRA
PPP3CC
EPHX2, CLU
SFRP1
ST18
NCOA2
MRPL13
FAM83H
C9ORF66 (DOCK8)
FREM1
CNTLN
FXN
SEC61B
PROSER2
EPHA10
ZNF644
SH3YL1
TTC21B
PRSS56
ACTR8
ZBTB38
PRKG2
RASGEF1B
SRSF12, PM20D2, GABRR2, UBE2J1, RRAGD
ARHGAP18
SHPRH
FKBP14, ADCYAP1R1
CACNA2D1
PPP1R9A
EPHX2
ZMAT4
ST18
LACTB2
FAM83H
C9ORF66 (DOCK8)
FREM1
TJP2, FAM189A2
TGFBR1
RGS3
PROSER2
TFAM
chr1:973501
chr1:38092723
chr1:91434335
chr1:113418415
chr1:200311910
chr1:207488004
chr1:208062973
chr1:219790221
chr2:301051
chr2:56011517
chr2:166627558
chr2:233385396
chr3:49211468
chr3:53837971
chr3:134086356
chr3:141093285
chr4:8461896
chr4:80827062
chr4:81903049
chr4:82422327
chr5:142720770
chr5:174720893
chr6:7317483
chr6:28162469
chr6:70446345
chr6:89918638
chr6:116446576
chr6:129820038
chr6:130354855
chr6:146245589
chr6:151620414
chr7:27937503_32236643
chr7:81400939
chr7:94731338
chr7:116365413
chr7:154406581
chr7:159093347
chr8:8961990
chr8:9807022
chr8:22538384
chr8:27466315
chr8:40726394
chr8:41103891
chr8:53362145
chr8:71420067
chr8:121622778
chr8:144811008
chr9:214501
chr9:14822828
chr9:17639458
chr9:71766593
chr9:101878622
chr9:116283516
chr10:11889837
chr10:60304864
Count
80
0
0
50
100
150
INF
Odds ratio

Figure 7

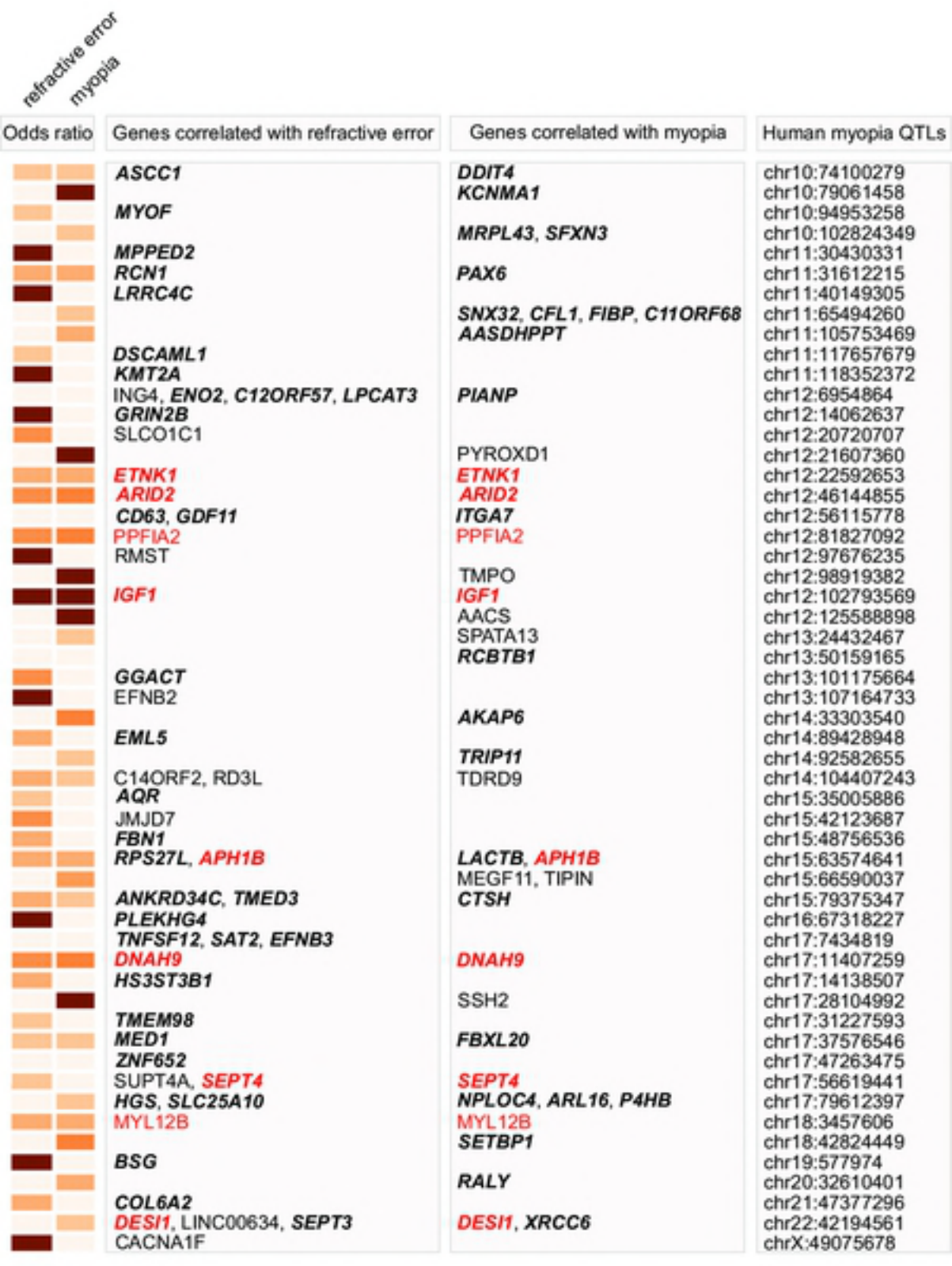
refractive error
myopia
Odds ratio
Genes correlated with refractive error
Genes correlated with myopia
Human myopia QTLs
ASCC1
MYOF
MPPED2
RCN1
LRRC4C
DSCAML1
KMT2A
ING4, ENO2, C12ORF57, LPCAT3
GRIN2B
SLCO1C1
ETNK1
ARID2
CD63, GDF11
PPFIA2
RMST
IGF1
GGACT
EFNB2
EML5
C14ORF2, RD3L
AQR
JMJD7
FBN1
RPS27L, APH1B
ANKRD34C, TMED3
PLEKHG4
TNFSF12, SAT2, EFNB3
DNAH9
HS3ST3B1
TMEM98
MED1
ZNF652
SUPT4A, SEPT4
HGS, SLC25A10
MYL12B
BSG
COL6A2
DESI1, LINC00634, SEPT3
CACNA1F
DDIT4
KCNMA1
MRPL43, SFXN3
PAX6
SNX32, CFL1, FIBP, C11ORF68
AASDHPPT
PIANP
PYROXD1
ETNK1
ARID2
ITGA7
PPFIA2
TMPO
IGF1
AACS
SPATA13
RCBTB1
AKAP6
TRIP11
TDRD9
LACTB, APH1B
MEGF11, TIPIN
CTSH
DNAH9
SSH2
FBXL20
SEPT4
NPLOC4, ARL16, P4HB
MYL12B
SETBP1
RALY
DESI1, XRCC6
chr10:74100279
chr10:79061458
chr10:94953258
chr10:102824349
chr11:30430331
chr11:31612215
chr11:40149305
chr11:65494260
chr11:105753469
chr11:117657679
chr11:118352372
chr12:6954864
chr12:14062637
chr12:20720707
chr12:21607360
chr12:22592653
chr12:46144855
chr12:56115778
chr12:81827092
chr12:97676235
chr12:98919382
chr12:102793569
chr12:125588898
chr13:24432467
chr13:50159165
chr13:101175664
chr13:107164733
chr14:33303540
chr14:89428948
chr14:92582655
chr14:104407243
chr15:35005886
chr15:42123687
chr15:48756536
chr15:63574641
chr15:66590037
chr15:79375347
chr16:67318227
chr17:7434819
chr17:11407259
chr17:14138507
chr17:28104992
chr17:31227593
chr17:37576546
chr17:47263475
chr17:56619441
chr17:79612397
chr18:3457606
chr18:42824449
chr19:577974
chr20:32610401
chr21:47377296
chr22:42194561
chrX:49075678
Count
0
80
0
50
100
150
INF
Odds ratio

Figure 8

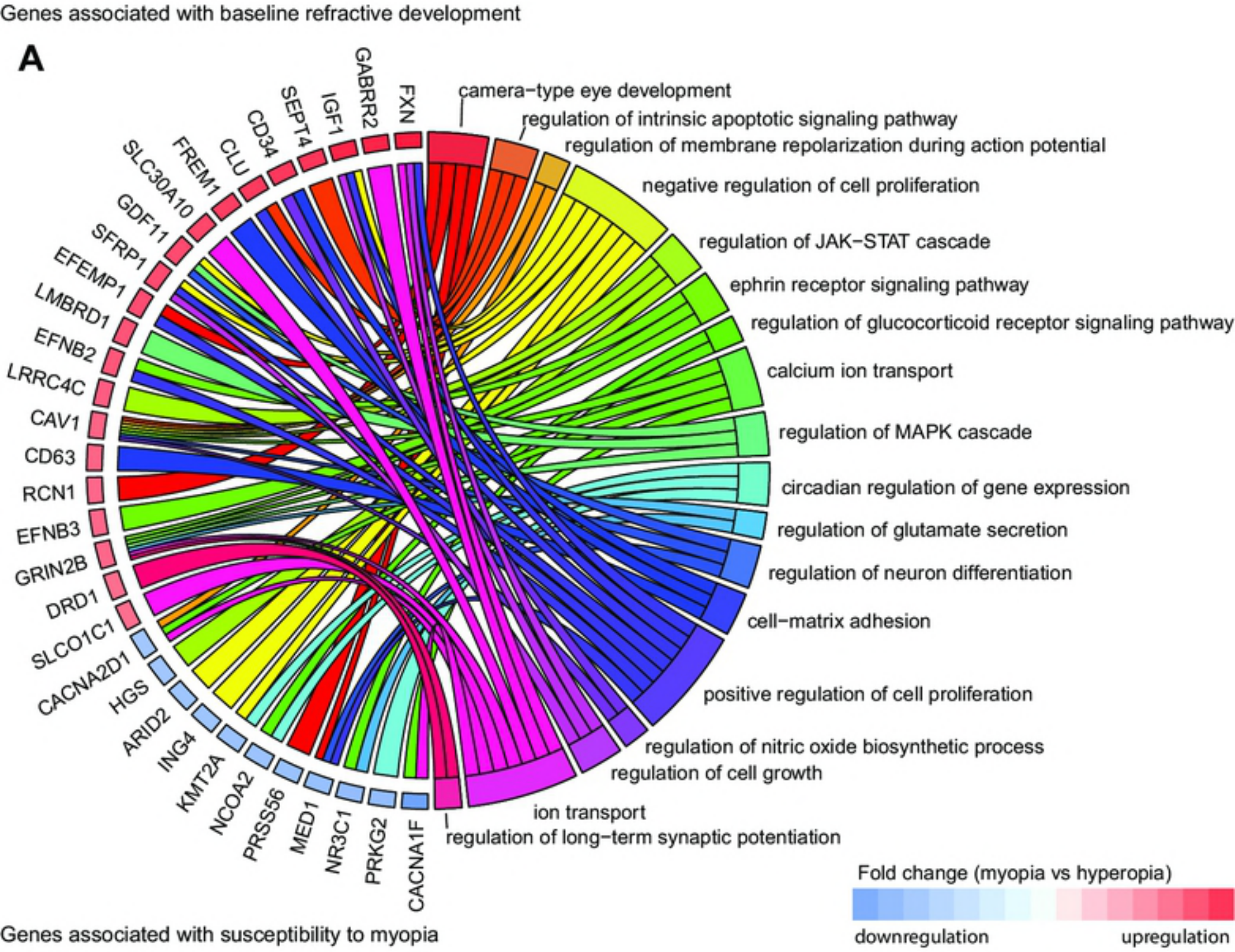
Genes associated with baseline refractive development
A
GABRR2
FXN
IGF1
SEPT4
CD34
CLU
FREM1
SLC30A10
GDF11
SFRP1
EFEMP1
LMBRD1
EFNB2
LRRC4C
CAV1
CD63
RCN1
EFNB3
GRIN2B
DRD1
SLCO1C1
CACNA2D1
HGS
ARID2
ING4
KMT2A
NCOA2
PRSS56
MED1
NR3C1
PRKG2
CACNA1F
camera−type eye development
regulation of intrinsic apoptotic signaling pathway
regulation of membrane repolarization during action potential
negative regulation of cell proliferation
regulation of JAK−STAT cascade
ephrin receptor signaling pathway
regulation of glucocorticoid receptor signaling pathway
calcium ion transport
regulation of MAPK cascade
circadian regulation of gene expression
regulation of glutamate secretion
regulation of neuron differentiation
cell−matrix adhesion
positive regulation of cell proliferation
regulation of nitric oxide biosynthetic process
regulation of cell growth
ion transport
regulation of long−term synaptic potentiation
Fold change (myopia vs hyperopia)
downregulation
upregulation

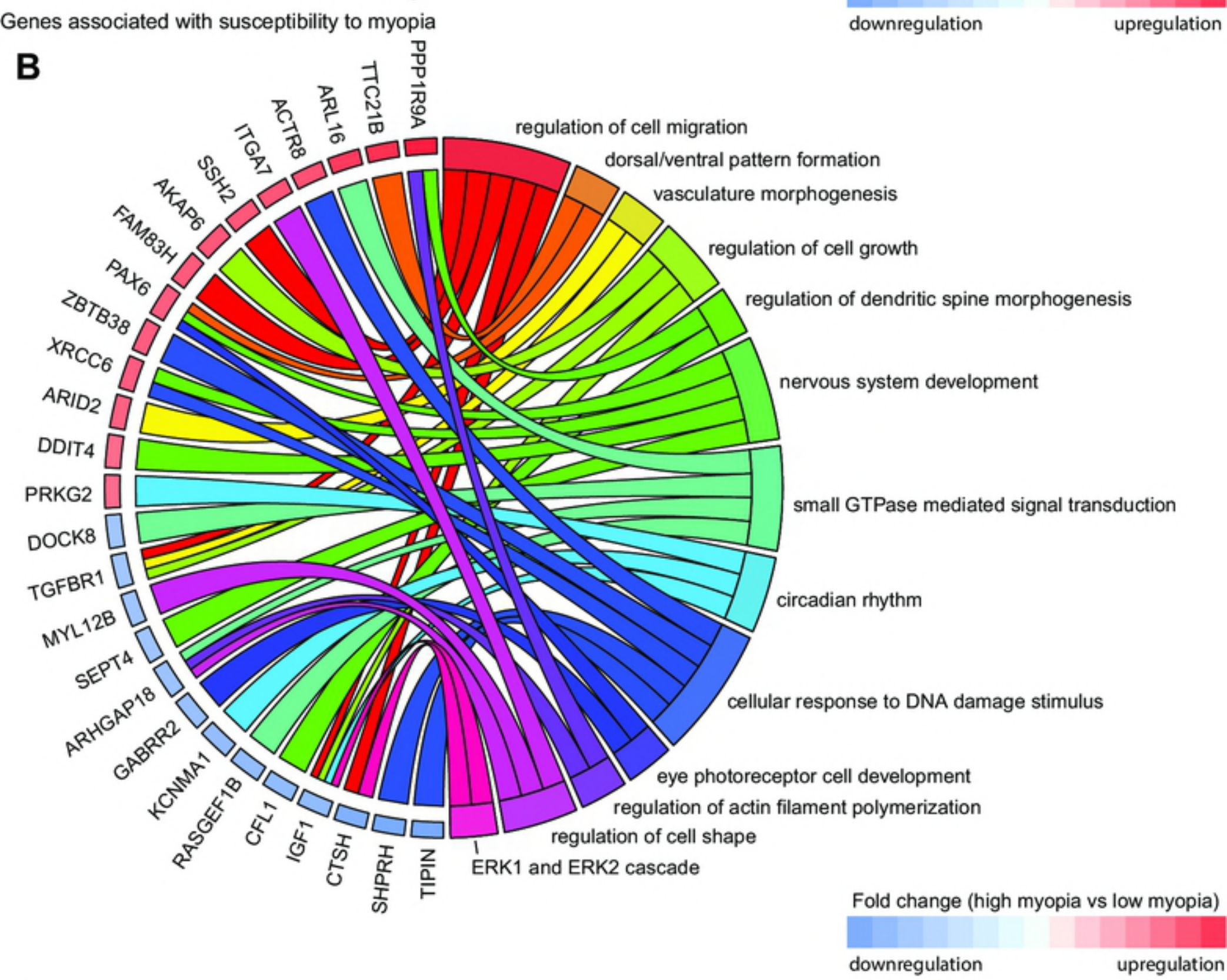
Genes associated with susceptibility to myopia
B
PPP1R9A
TTC21B
ARL16
ACTR8
ITGA7
SSH2
AKAP6
FAM83H
PAX6
ZBTB38
XRCC6
ARID2
DDIT4
PRKG2
DOCK8
TGFBR1
MYL12B
SEPT4
ARHGAP18
GABRR2
KCNMA1
RASGEF1B
CFL1
IGF1
CTSH
SHPRH
TIPIN
regulation of cell migration
dorsal/ventral pattern formation
vasculature morphogenesis
regulation of cell growth
regulation of dendritic spine morphogenesis
nervous system development
small GTPase mediated signal transduction
circadian rhythm
cellular response to DNA damage stimulus
eye photoreceptor cell development
regulation of actin filament polymerization
regulation of cell shape
ERK1 and ERK2 cascade
Fold change (high myopia vs low myopia)
downregulation
upregulation

Figure 9

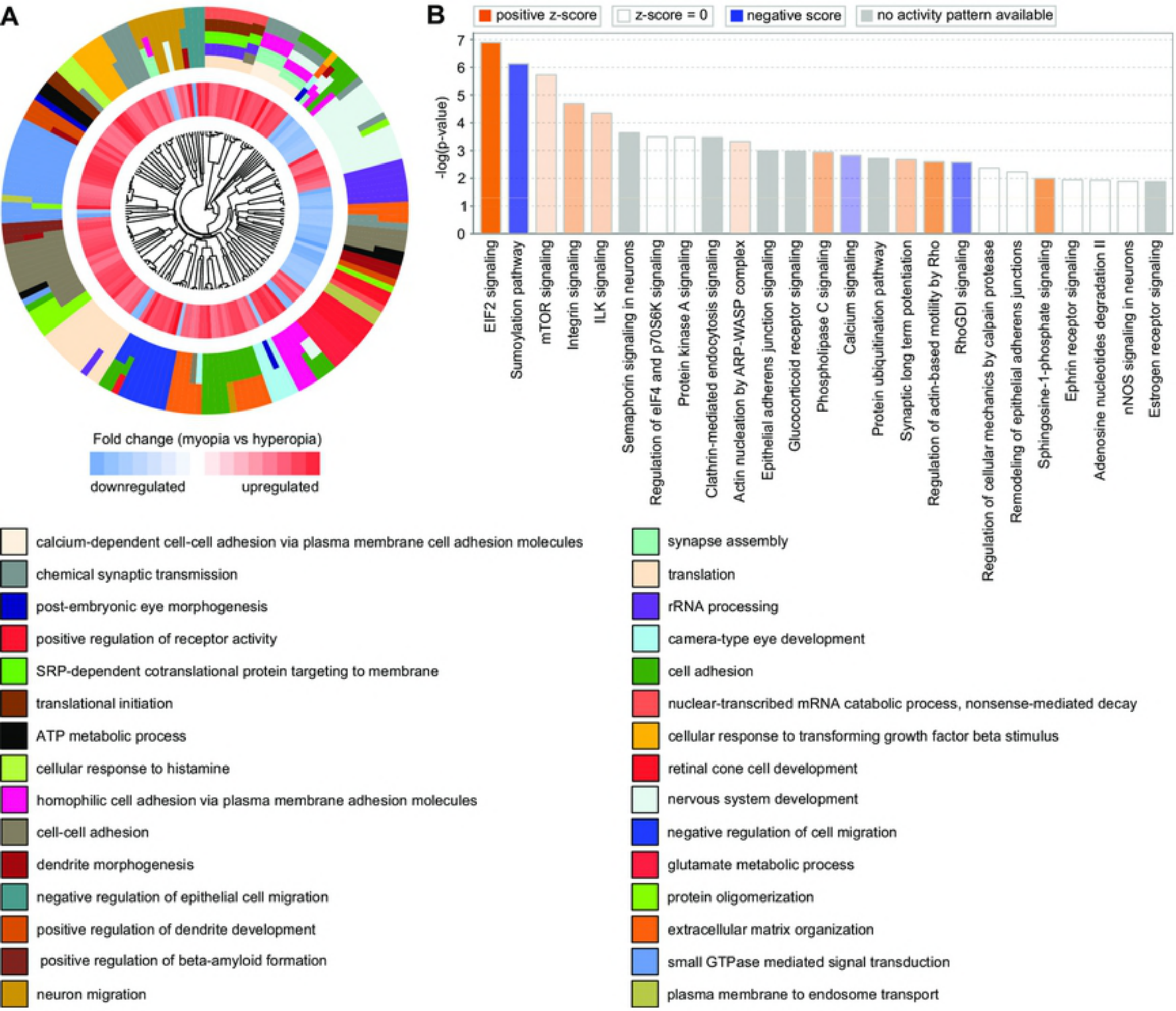
A
Fold change (myopia vs hyperopia)
downregulated
upregulated
B
positive z-score
z-score = 0
negative score
no activity pattern available
-log(p-value)
0
1
2
3
4
5
6
7
EIF2 signaling
Sumoylation pathway
mTOR signaling
Integrin signaling
ILK signaling
Semaphorin signaling in neurons
Regulation of eIF4 and p70S6K signaling
Protein kinase A signaling
Clathrin-mediated endocytosis signaling
Actin nucleation by ARP-WASP complex
Epithelial adherens junction signaling
Glucocorticoid receptor signaling
Phospholipase C signaling
Calcium signaling
Protein ubiquitination pathway
Synaptic long term potentiation
Regulation of actin-based motility by Rho
RhoGDI signaling
Regulation of cellular mechanics by calpain protease
Remodeling of epithelial adherens junctions
Sphingosine-1-phosphate signaling
Ephrin receptor signaling
Adenosine nucleotides degradation II
nNOS signaling in neurons
Estrogen receptor signaling
calcium-dependent cell-cell adhesion via plasma membrane cell adhesion molecules
chemical synaptic transmission
post-embryonic eye morphogenesis
positive regulation of receptor activity
SRP-dependent cotranslational protein targeting to membrane
translational initiation
ATP metabolic process
cellular response to histamine
homophilic cell adhesion via plasma membrane adhesion molecules
cell-cell adhesion
dendrite morphogenesis
negative regulation of epithelial cell migration
positive regulation of dendrite development
positive regulation of beta-amyloid formation
neuron migration
synapse assembly
translation
rRNA processing
camera-type eye development
cell adhesion
nuclear-transcribed mRNA catabolic process, nonsense-mediated decay
cellular response to transforming growth factor beta stimulus
retinal cone cell development
nervous system development
negative regulation of cell migration
glutamate metabolic process
protein oligomerization
extracellular matrix organization
small GTPase mediated signal transduction
plasma membrane to endosome transport

Figure 10

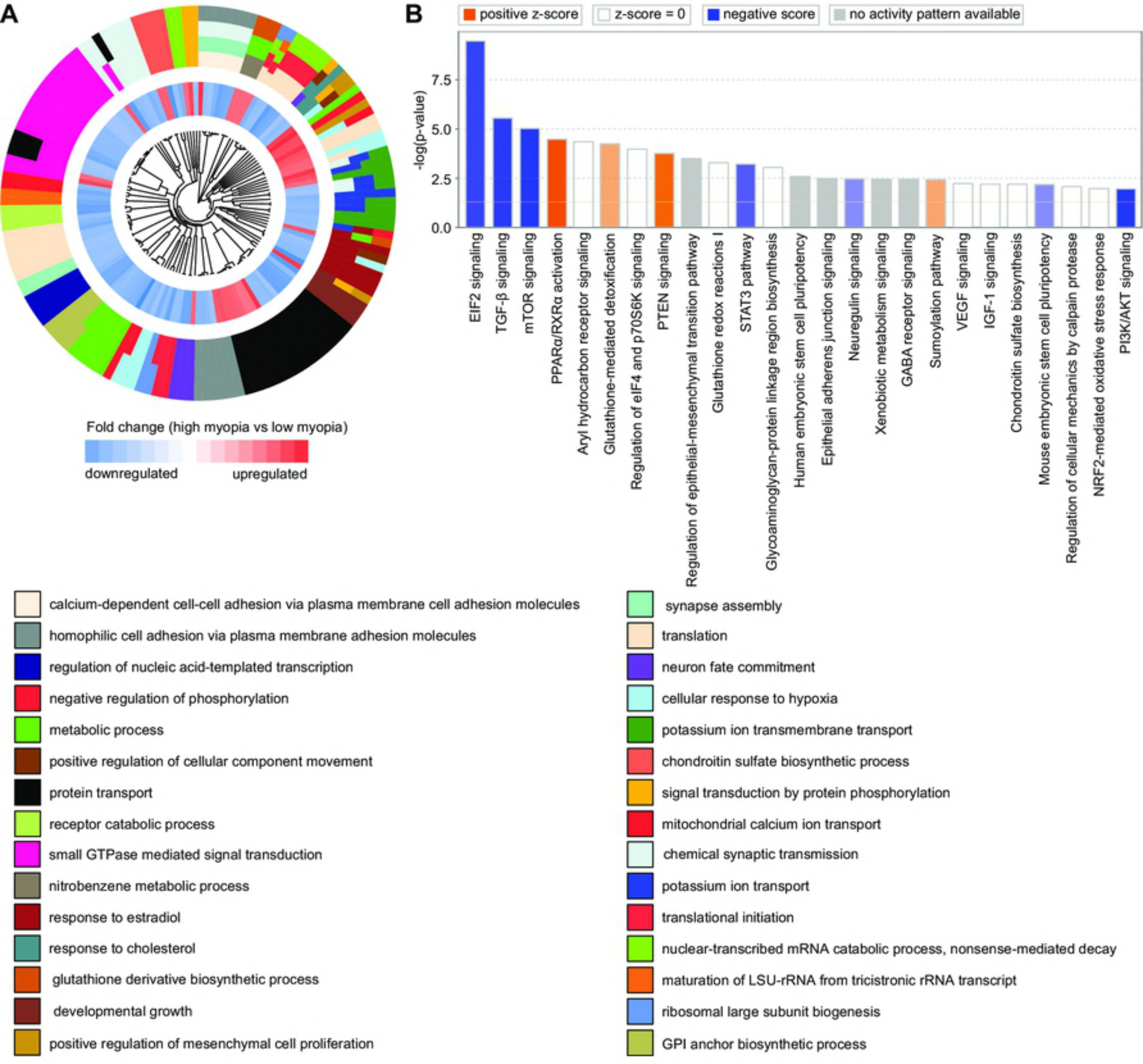
A
Fold change (high myopia vs low myopia)
downregulated
upregulated
B
positive z-score
z-score = 0
negative score
no activity pattern available
-log(p-value)
7.5
5.0
2.5
0.0
EIF2 signaling
TGF-β signaling
mTOR signaling
PPARα/RXRα activation
Aryl hydrocarbon receptor signaling
Glutathione-mediated detoxification
Regulation of eIF4 and p70S6K signaling
PTEN signaling
Regulation of epithelial-mesenchymal transition pathway
Glutathione redox reactions I
STAT3 pathway
Glycoaminoglycan-protein linkage region biosynthesis
Human embryonic stem cell pluripotency
Epithelial adherens junction signaling
Neuregulin signaling
Xenobiotic metabolism signaling
GABA receptor signaling
Sumoylation pathway
VEGF signaling
IGF-1 signaling
Chondroitin sulfate biosynthesis
Mouse embryonic stem cell pluripotency
Regulation of cellular mechanics by calpain protease
NRF2-mediated oxidative stress response
PI3K/AKT signaling
calcium-dependent cell-cell adhesion via plasma membrane cell adhesion molecules
homophilic cell adhesion via plasma membrane adhesion molecules
regulation of nucleic acid-templated transcription
negative regulation of phosphorylation
metabolic process
positive regulation of cellular component movement
protein transport
receptor catabolic process
small GTPase mediated signal transduction
nitrobenzene metabolic process
response to estradiol
response to cholesterol
glutathione derivative biosynthetic process
developmental growth
positive regulation of mesenchymal cell proliferation
synapse assembly
translation
neuron fate commitment
cellular response to hypoxia
potassium ion transmembrane transport
chondroitin sulfate biosynthetic process
signal transduction by protein phosphorylation
mitochondrial calcium ion transport
chemical synaptic transmission
potassium ion transport
translational initiation
nuclear-transcribed mRNA catabolic process, nonsense-mediated decay
maturation of LSU-rRNA from tricistronic rRNA transcript
ribosomal large subunit biogenesis
GPI anchor biosynthetic process

Figure 11